

Online Research @ Cardiff

This is an Open Access document downloaded from ORCA, Cardiff University's institutional repository: <https://orca.cardiff.ac.uk/id/eprint/97792/>

This is the author's version of a work that was submitted to / accepted for publication.

Citation for final published version:

Amoroso, Angelo James ORCID: <https://orcid.org/0000-0002-7601-5482>, Fallis, Ian Andrew ORCID: <https://orcid.org/0000-0001-7361-0182> and Pope, Simon J. A. ORCID: <https://orcid.org/0000-0001-9110-9711> 2017. Chelating agents for radiolanthanides: applications to imaging and therapy. Coordination Chemistry Reviews 340 , pp. 198-219. 10.1016/j.ccr.2017.01.010 file

Publishers page: <http://dx.doi.org/10.1016/j.ccr.2017.01.010>
<<http://dx.doi.org/10.1016/j.ccr.2017.01.010>>

Please note:

Changes made as a result of publishing processes such as copy-editing, formatting and page numbers may not be reflected in this version. For the definitive version of this publication, please refer to the published source. You are advised to consult the publisher's version if you wish to cite this paper.

This version is being made available in accordance with publisher policies.

See

<http://orca.cf.ac.uk/policies.html> for usage policies. Copyright and moral rights for publications made available in ORCA are retained by the copyright holders.



Chelating agents for radiolanthanides: applications to imaging and therapy

Angelo J. Amoroso,* Ian A. Fallis,* Simon J.A. Pope*

School of Chemistry, Main Building, Cardiff University, Park Place,
Cardiff, UK CF10 3AT

Email: amorosoaj@cardiff.ac.uk, fallis@cardiff.ac.uk, popesj@cardiff.ac.uk

Keywords: radiolanthanides, chelators, imaging, therapy, theranostics

Contents

1. Introduction
2. Properties of the radiolanthanides
3. Coordination chemistry of radiolanthanides
 - 3.1. Complexes based on (poly)aminophosphonic acids
 - 3.1.1. Acyclic ligand derivatives
 - 3.1.2. Macrocyclic ligand derivatives
 - 3.2. Complexes based on (poly)aminocarboxylic acids
 - 3.3. Complexes that incorporate porphyrins
4. Radiolanthanides labelled with peptides
5. Complexes for radioimmunotherapy applications
6. Radiolanthanides linked to, or incorporated into, nanostructures and nanoparticles
7. Future prospects and untapped potential

1. Introduction

In this review, we examine the chelating ligand design and coordination complexes of radioactive lanthanide isotopes. Where appropriate, discussion is placed in the context of the radioimaging and radiotherapeutic applications of such complexes. This, of course, is a very large subject area, and we have therefore selected, where possible, those examples that illustrate the underlying coordination chemistry features of the ligand systems in question, and how they are suitable for the target applications. In some instances, we shall refer to clinical work, both as a means of illustrating the translational potential of radiolanthanide coordination chemistry systems and to provide readers with an appreciation of the ever-expanding application areas of these materials.

The use of radioisotopes in diagnostic imaging science is currently dominated by a relatively small number of isotopes. These include the single gamma photon emitting isotopes $^{99\text{m}}\text{Tc}$, ^{67}Ga and ^{111}In (see Table 1) that are employed in gamma photography techniques,¹ such as ^{67}Ga scintigraphy (a ‘gallium’ scan) and single-photon emission computed tomography (SPECT); currently $^{99\text{m}}\text{Tc}$ accounts for approximately 80% of all nuclear medicine procedures where ($^{99\text{m}}\text{Tc}$ -tetrofosmin for cardiac perfusion). In positron emission tomography (PET), β^+ emission followed by electron annihilation results in the emission of collinear gamma rays, a method dominated by widely available ^{18}F tracers (e.g. ^{18}F -fluorodeoxyglucose is used as a metabolic indicator). The decay properties of a given tracer are of course of paramount importance in developing viable applications. For example, when considering the suitability of an isotope as a potential PET tracer, many factors must be examined. Of central importance is the β^+ emission energy (not to be confused with the 511 keV

annihilation energy) which determines the range of the emitted positrons (mean free paths) in condensed matter, and hence set a limit to the resolution of PET scans. To illustrate this we can compare the well documented examples of ^{18}F and ^{15}O , which possess maximum emission energies of 675 and 1720 keV respectively, with the corresponding FWTM (full width at tenth of maximum) scatter values of 1.03 mm and 4.14 mm.² The lower 'scatter' of ^{18}F results in considerably better spatial resolution in PET imaging. Whilst comparable studies are to date lacking for the radiolanthanides, it is reasonable to predict that β^+ isotopes with energies in these energy ranges would yield comparable results, and clearly isotopes with lower energies would yield better imaging performance.

While the clear majority of current clinical diagnostic imaging and radiotherapy is dominated by a small number of isotopes (e.g. Table 1) the ever-increasing access to 'new' isotopes have expanded the medical radiochemist's repertoire of available materials and modalities. To a large extent, this expansion is being driven by the availability of new metal isotopes and hence the development of new diagnostics, therapies, and the emerging science of theranostic agents, is one in which the coordination chemist is set to play an important role. Lanthanide radioisotopes also find extensive use as therapeutic agents, with a relatively small number of potential systems exploited in this respect.³ Here, the β -emitters dominate, with ^{153}Sm and ^{177}Lu (and the group 3 element ^{90}Y , often referred to as a pseudo lanthanide) commonly studied with the emission energies of these species sufficient to allow significant tissue penetration. In this context, Neves *et al.* reviewed the potential of unexploited radionuclides, including a number of radiolanthanides, a decade ago.⁴

| Radionuclide | Half-life | Decay mode(s) | Uses |
|-------------------|-----------|---------------------------------------------------------------|---------|
| ¹⁸ F | 1.83 h | β^+ (633.5 keV), EC / γ (511 keV) | Imaging |
| ⁶⁴ Cu | 12.70 h | β^- (578 keV, 40%), β^+ (650 keV, 19%), EC (41%) | Imaging |
| ⁶⁷ Ga | 3.26 d | EC / γ (93 keV, 37%; 184 keV, 20%; 300 keV, 17%) | Imaging |
| ⁶⁸ Ga | 1.13 h | β^+ (830 keV, 90%), EC (10%) | Imaging |
| ⁸² Rb | 1.27 min | β^+ (3.379 keV, 96%), EC (4%) / γ (511, 767 keV) | Imaging |
| ⁹⁰ Y | 2.67 d | β^- (2.282 MeV) | Therapy |
| ^{99m} Tc | 6.01 h | IT (142 keV) | Imaging |
| ¹¹¹ In | 2.80 d | EC / γ (171, 245 keV) | Imaging |
| ¹³¹ I | 8.04 d | β^- (0.971 MeV) / γ (80, 284, 364, 637 keV) | Therapy |

Table 1. Radioactive properties of selected isotopes commonly used in nuclear medicine. EC = electron capture; IT = isomeric transition. Data is drawn from reference [5].

This review is structured to provide the reader with an overview of the different radiolanthanide isotopes (and their potential in an imaging and therapeutic context) as well as the different classes of chelating ligands that have been thus far investigated in the coordination chemistry of radiolanthanides. We have limited our discussion to examples from the literature that demonstrate the breadth of the topic, particularly in a coordination chemistry context, and point to future directions for this multidisciplinary topic.

2. Radiolanthanide isotopes

Although there are hundreds of radiolanthanide isotopes described in the literature, we have chosen to focus upon those radiolanthanide species for which some form of descriptive coordination chemistry is available. The radiolanthanides discussed in this review are summarised in Table 2.

| Radionuclide | Half-life | Decay mode(s) | Uses / Potential Uses |
|-------------------|----------------|-----------------------------------------------------------------------------|-----------------------------|
| ¹³⁴ La | 6.5 m | β^+ (63%, 2.67 MeV), EC (37%) / γ (605 keV) | Therapy Tracer Tracer |
| ¹⁴⁰ La | 1.678 d | β^- (3.76 MeV) | |
| ¹³⁴ Ce | 3.16 d | EC (500 keV) / γ (130, 162, 605 keV) | |
| ¹⁴¹ Ce | 32.5 d | β^- (69%, 436 keV; 31%, 581 keV) | |
| ¹⁴⁴ Ce | 284.6d | β^- (185, 318 keV) | |
| ¹⁴⁰ Pr | 3.39 m | β^+ (51%, 2.37 MeV), EC (49%) / γ (307, 1597 keV) | Therapy |
| ¹⁴³ Pr | 13.58 d | β^- (933 keV), γ (742 keV) | |
| ¹⁴⁴ Pr | 17.28 m | β^- (98%, 2.996 MeV) | |
| ¹⁴⁰ Nd | 3.37 d | EC (220 keV) | Imaging |
| ¹⁴⁷ Nd | 10.98 d | β^- (895 keV), γ (531, 91 to 686 keV) | Therapy |
| ¹⁴⁹ Pm | 2.21 d | β^- (1.071 MeV), γ (286, 591, 859 keV) | Therapy |
| ¹⁵³ Sm | 1.929 d | β^- (808 keV) | Therapy (bone) |
| ¹⁴⁹ Gd | 9.2 d | EC (1.32 MeV), γ (150, 296, 347 keV) | Imaging |
| ¹⁴⁹ Tb | 4.13 h | α (16%, 3.97 MeV), β^+ (4%, 1.8 MeV) | |
| ¹⁵² Tb | 17.5 d | EC (80%, 2.8 MeV), β^+ (20%, 2.5 MeV) | |
| ¹⁵⁵ Tb | 5.3 d | EC (0.82 MeV), γ (87, 105 keV) | |
| ¹⁶¹ Tb | 6.91 d | β^- (593 keV), γ (26, 49, 75 keV) | |
| ¹⁵⁷ Dy | 8.1 h | EC (1.34 MeV) | Imaging |
| ¹⁶⁵ Dy | 2.33 h | β^- (1.286 MeV), γ (95 keV) | Therapy |
| ¹⁶⁶ Dy | 3.40 d | β^- (486 keV), γ (28, 83 keV) | Therapy |
| ¹⁶¹ Ho | 2.48 h | EC (859 keV) | Imaging |
| ¹⁶⁶ Ho | 1.12 d | β^- (51%, 1.855 MeV; 49% 1.776 MeV), γ (83 keV, 1.38 MeV) | Therapy |
| ¹⁶⁰ Er | 1.191 d | EC (330 keV) | Imaging |
| ¹⁶⁵ Er | 10.36 h | EC (376 keV) | Therapy |
| ¹⁶⁹ Er | 9.4 d | β^- (350 keV), γ (111, 112 keV) | Therapy |
| ¹⁷¹ Er | 0.31 d | β^- (1.49 MeV), γ (111, 296, 308 keV) | |
| ¹⁶⁷ Tm | 9.24 d | EC (748 keV) | |
| ¹⁷⁰ Tm | 128.6 d | β^- (99.8 %, 883, 968 keV) | |
| ¹⁶⁶ Yb | 2.36 d | EC (300 keV) | |
| ¹⁷⁵ Yb | 4.19 d | β^- (73%, 466 keV; 21%, 71 keV; 6%, 353 keV), γ (114, 396 keV) | Therapy |
| ¹⁷⁷ Lu | 6.71 d | β^- (498 keV), γ (113, 208 keV) | Therapy |

Table 2. Radioactive properties of selected radiolanthanide isotopes. Data is drawn from reference [4]. Those entries in bold are in clinical use.

Readers should exercise caution when digesting the literature in this subject area as the nuclear data characteristics cited can sometimes be inconsistent. The data in Table 2 has been drawn largely from reference^{5a} and corroborated by referring to nuclear data sheets at the National Nuclear Data Center, Brookhaven National Laboratory.^{5b}

A number of radiolanthanides are well known and are now widely investigated for a variety of applications (see later sections). In the following section, we wish to highlight some relevant isotopes that are in the infancy of their development. The radiosynthesis of these radiolanthanides is often complex and expensive, and whilst we have alluded to some of the radiosynthesis procedures below, a general discussion is beyond the scope of this article.

¹³⁴Ce/¹³⁴La

Despite reports of the Auger electron and positron emitting ¹³⁴Ce/¹³⁴La isotopes⁶ (half-lives: 3.16 d, 6.45 min) there are no reports of the development of the use of this PET isotope in preclinical experiments. While the coordination chemistry of these early lanthanides is slightly varied from the later lanthanides,⁷ ¹³⁴Ce/¹³⁴La could find similar utility as other more familiar lanthanide isotopes. ¹³⁴Ce was produced from a natural abundance lanthanum metal disc bombarded with 70-72 MeV protons. The product was dissolved using NaBrO₃ and HNO₃ and extracted into methylisobutylketone. Significant ¹³⁵Ce was produced meaning that samples were initially left for two days for the by-product to decay.

¹⁴⁰La

^{140}La is a fission product that is a beta emitter with a half-life of 1.68 days. It decays to the stable ^{140}Ce isotope. Kobayashi *et al.* have reported its inclusion within a fullerene framework and shown the biodistribution of the agent within a rat.⁸ The energy of the beta decay is 3.76 MeV with the major gamma energy transition (γ_{28}) at 1.596 MeV which is intermediate to those of ^{90}Y (2.28 MeV) and ^{166}Ho (711 keV). One point of concern may be the lower thermodynamic stability of lanthanum complexes in comparison to other smaller lanthanide ions.

$^{140}\text{Nd}/^{140}\text{Pr}$

Zhernosekov *et al.* have reported the production of ^{140}Nd up to 200 MBq.⁹ The nuclear processes $^{\text{nat}}\text{Ce}(3\text{He}, \text{xn})$ and $^{141}\text{Pr}(\text{p}, 2\text{n})$ were investigated and the chemical isolation of $^{140}\text{Nd}(\text{III})$ from $\text{Ce}(\text{III})$ and $\text{Pr}(\text{III})$ was performed by cation-exchange chromatography with a decontamination factor from the respective target material of $\sim 10^8$ and 7×10^5 . A $^{140}\text{Nd}/^{140}\text{Pr}$ generator system was developed utilising the DOTA (1,4,7,10-tetraazacyclododecane-1,4,7,10-tetraacetic acid) complex of ^{140}Nd to isolate the positron emitter, ^{140}Pr (half-life = 3.39 min). The generator showed high elution yield and high chemical and radiochemical stability, with the activity of the daughter nuclide sufficient for *in vivo* PET investigations. However, it was noted that the use of $^{140}\text{Nd}/^{140}\text{Pr}$ as an *in vivo* radionuclide generator, needs more consideration, especially when one considers the use of the ^{140}Nd DOTA complex used to generate free ^{140}Pr . It was suggested that ligands other than DOTA should be utilised for this purpose.⁹

^{141}Ce

^{141}Ce has been commonly used in tracer studies. For example, in older literature the long half-life of ^{141}Ce (β^- , half-life = 32.5 d) made it attractive as a tracer when loaded

into porous di-vinyl benzene polystyrene microspheres (typically 5 – 15 μm diameter) as a tracer to examine blood flow and other vascular functions.^{10,11,12} ^{141}Ce has even found applications in plant ‘imaging’, being employed as a tracer in the growth of horseradish¹³ and tea plants.¹⁴ The production of ^{141}Ce -ceria and nanoceria powders as potential imaging and therapeutic agents has been examined.¹⁵

$^{144}\text{Ce}/^{144}\text{Pr}$ generator

^{144}Ce is a fission product, undergoing radioactive decay with a half-life of 284.1 d via β^- emission to ^{144}Pr . ^{144}Pr has a half-life of 17.3 min and decays via β^- emission to ^{144}Nd . The long half-life of ^{144}Ce would appear to preclude any useful therapeutic applications. However, the rapid separation of these isotopes has been achieved by absorbing them to alumina and, under oxidizing conditions, Ce(IV) is retained while Pr(III) may be eluted. The process was found to be quantitative.¹⁶

^{149}Tb , ^{152}Tb , ^{155}Tb , ^{160}Tb , ^{161}Tb

^{149}Tb (half-life = 4.1 h) is a dual alpha emitter (3.97 MeV, 16.7%) and PET isotope (730 keV, 7.1%) making it a potential α -PET radiotheranostic.¹⁷ ^{152}Tb (half-life = 17.5 h) is a positron emitter (1.08 MeV, 17%) and ^{155}Tb (half-life = 5.32 days) decays by EC (100%) and is suitable for SPECT. ^{161}Tb (half-life = 6.9 days) is a low energy beta emitter (0.15 MeV) and also produces low energy photons making it suitable for therapy as well as SPECT. The majority of these Tb isotopes can be made at ISOLDE (isotope mass separator on-line facility)/CERN¹⁸ by the radiation of a Ta-Re target and mass separation of the isotopes, except for ^{161}Tb which has been synthesised by the neutron irradiation of ^{160}Gd .¹⁹

¹⁷²Hf/¹⁷²Lu generator

The ¹⁷²Hf radionuclide (half-life = 1.8 y) decays by EC to ¹⁷²Lu (half-life = 6.7 d), which subsequently decays to stable ¹⁷²Yb. ¹⁷²Lu emits gamma rays ranging from 79 to 1622 keV. The generator has been used for analytical applications,²⁰ but has yet to find applications as a therapeutic agent, and coordination complexes of ¹⁷²Lu have not yet been reported.

The separation chemistry of radiolanthanides is clearly a challenging subject area and Liu *et al.* have reported an amide-based tripodal ligand (6-[2-(2-diethylamino-2-oxoethoxy)ethyl]-N,N,12-triethyl-11-oxo-3,9-dioxo-6,12-diazatetradecanamide), shown in Fig. 1, that acts as an extractant for selected radiolanthanide ions.²¹ Using a multitracer solution containing twelve radioactive rare earth nuclides (¹⁴⁰La, ¹⁴¹Ce, ¹⁴⁷Nd, ¹⁴⁸Pm, ¹⁴⁷Eu, ¹⁴⁹Gd, ¹⁵³Tb, ¹⁶⁰Er, ¹⁶⁷Tm, ¹⁶⁶Yb and ¹⁷⁷Lu) they were able to demonstrate high extractability and excellent cation selectivity towards ¹⁴⁷Pm, which possessed the highest extraction equilibrium constant, $\log K_{\text{ex}} = 10.65$. The authors report X-ray structural data for Ln(III) complexes of this ligand with picrate (picric acid = 2,4,6-trinitrophenol) as co-ligand, with the coordination sphere best described as a monocapped distorted square prism or antiprism. However, with a modest stability, it is unlikely that Ln(III) complexes of this ligand could be used for some of the biological applications that are discussed in this review.

3. Coordination chemistry of radiolanthanides

The coordination chemistry, physical properties, and applications of lanthanide ions are vast and we encourage readers to utilise the number of general reviews on lanthanides,²² which describe the wide breadth of ligand design, as well as a more focused review discussing their breadth of potential in cancer diagnosis and therapy.²³ Also of relevance, are a number of previous reviews that summarise therapeutic radiopharmaceuticals (which includes some coverage of ^{153}Sm and ^{166}Ho),²⁴ prospective theranostics,²⁵ as well more specific topics such as radiopharmaceuticals for palliative care of patients with castration-resistant prostate cancer metastatic to bone, where ^{153}Sm has particular relevance.²⁶ While the breadth of ^{177}Lu application to the development of radiopharmaceuticals has been recently documented in detail,²⁷ we will highlight some (topical) examples of its coordination chemistry and application.

Finally, it is obvious from the literature that there are inconsistencies when naming the many chelating ligands referred to within this review. Thus, 1,4,7,10-tetraazacyclododecane-1,4,7,10-tetraacetic acid is frequently referred to as its synonym, DOTA, but also sometimes referred to as H_4DOTA (to reflect the correct protonation state of the free ligand). For consistency with the majority of the literature reports we will adopt the use of DOTA as the abbreviation and assume this naming protocol for all other relevant ligands throughout this review.

3.1. Complexes based on (poly)aminophosphonic acids

Radiopharmaceuticals based on (poly)aminophosphonic acids has been a primary area of development in the last two decades, often specifically targeting bone therapy and imaging. A wide range of radionuclides have been investigated with such ligand systems, many of which (^{99m}Tc , ^{68}Ga , ^{227}Th , ^{228}Ac , ^{212}Bi , ^{188}Re) are beyond the realm of this current review, but are discussed in the context of (poly)aminophosphonic acids elsewhere.²⁸ Specific review articles have also focused upon the targeted treatment of bone metastases using phosphonate-based ligands²⁹ and a broad range of radionuclides.³⁰

3.1.1. Acyclic ligand derivatives

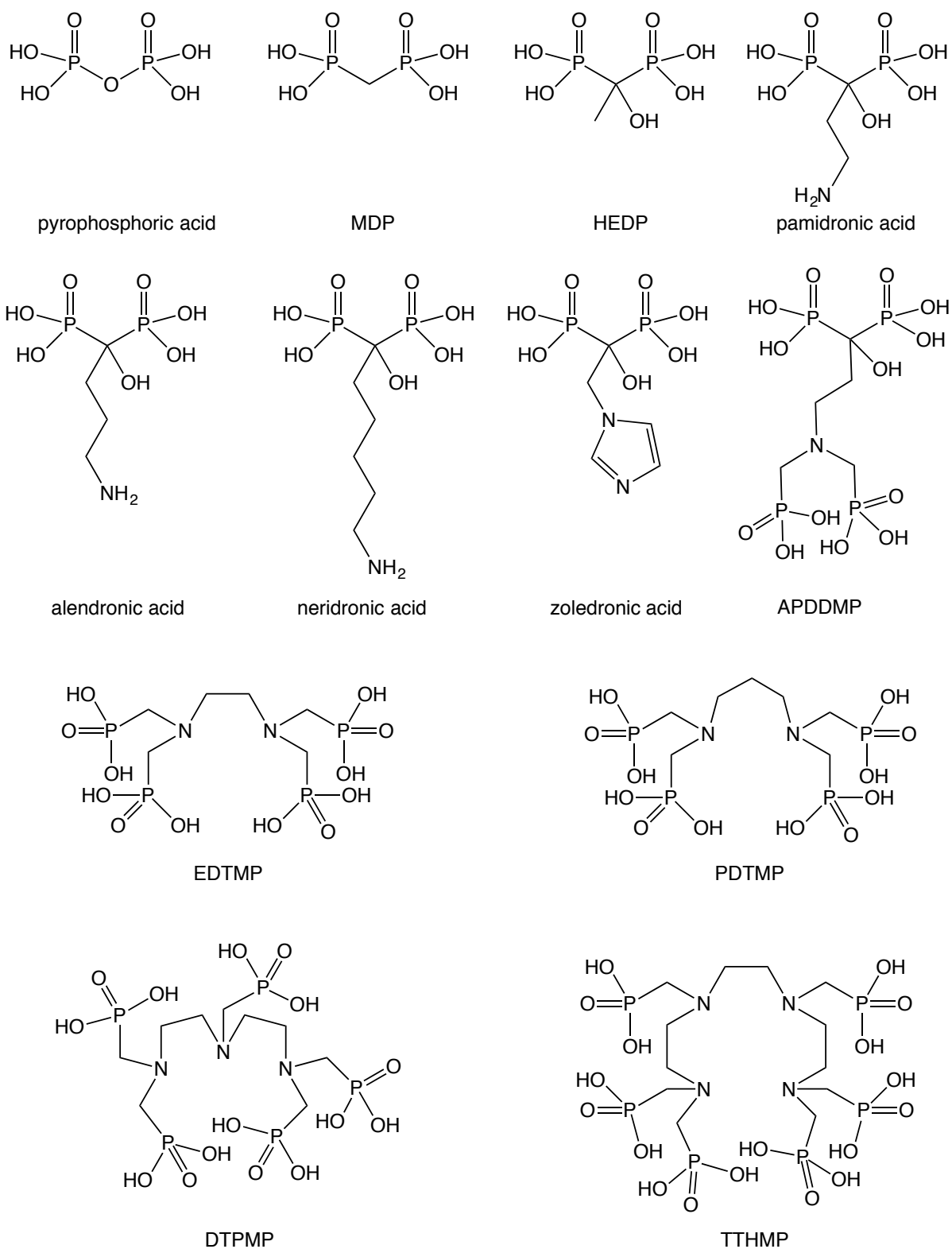


Figure 2. Examples of acyclic ligands based on aminophosphonic acids.

Although not an aminophosphonic acid, the structurally simplest biposphonic acid derivative is pyrophosphonic acid (Fig. 2). The complexation of this ligand has been reported with ^{177}Lu , where the complex was obtained using a ligand:metal ratio of 60:1. No precise information on the complex speciation was given and no corresponding work with natural Lu(III) was detailed. Preliminary animal imaging studies showed high skeletal uptake of ^{177}Lu .³¹

Ethylenediaminetetramethylenephosphonic acid (EDTMP, Fig. 2) has been one of the most widely studied aminophosphonate based ligands. This is primarily due to the development of ^{153}Sm -EDTMP (also known as samarium lexidronam, or Quadramet) as an intravenous treatment for cancer-induced pain which has spread to the bone.³² Remarkably, given the clinical importance of this compound, the first solid state structural characterisation (Fig. 3) of the Sm(III) complex of EDTMP was only recently reported using EXAFS,³³ confirming the assumptions (EDTMP acts as a 6-coordinate ligand) previously made about the solution state speciation and ligand binding mode to Sm(III). The thermal analyses of Ln(III) complexes of EDTMP have also been reported in detail.³⁴

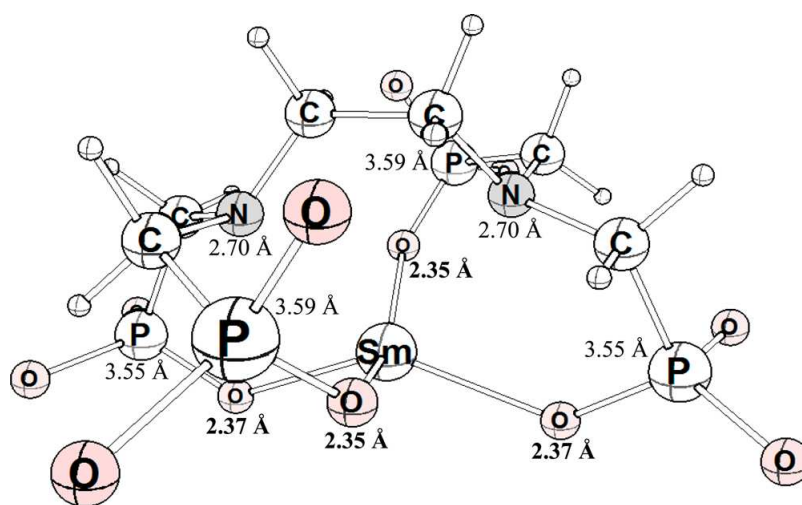


Figure 3. Geometry optimized DFT structure of $[\text{Sm}(\text{EDTMP})]^{5-}$, used to fit the EXAFS data. Bonds to the remote N atoms, beyond 2.7 Å, are not explicitly drawn. Additional coordination from solvent is not explicitly modeled. Relevant $\text{Sm}\cdots\text{X}$ atom separations

are shown with the distance closest to the atom of interest (Sm–O bond lengths are shown in bold). Reprinted with permission from Yang *et al.*, *Mol. Pharmaceutics* **2015**, 12, 4108–4114. Copyright 2015 American Chemical Society.

Stability constants and dissociation rates for Sm(III) and Y(III) complexes of EDTMP are known:³⁵ Sm-EDTMP with $\log K_{ML} = 20.71$ and for Y-EDTMP with $\log K_{ML} = 19.19$. Interestingly, in a modelled blood plasma medium the Sm(III) complex is present as the (mono-protonated) form $[\text{Sm}(\text{HEDTMP})\text{Ca}]^{2-}$. In related studies on Eu-EDTMP it was shown³⁶ that the anionic carbonate complex $[\text{Eu}(\text{EDTMP})(\text{CO}_3)]^{7-}$ was thermodynamically stable with low dissociation constants. The authors report the X-ray crystal structure (Fig. 4) which shows an 8-coordinate complex, with the EDTMP acting as a 6-coordinate ligand and carbonate as a bidentate (no water is in the coordination sphere). It is noteworthy that these results may provide insight into the uptake mechanism of ^{153}Sm -EDTMP. Work has also investigated the ^{152}Eu and long-lived ^{154}Eu radio-contaminants that are present in ^{153}Sm -EDTMP.³⁷

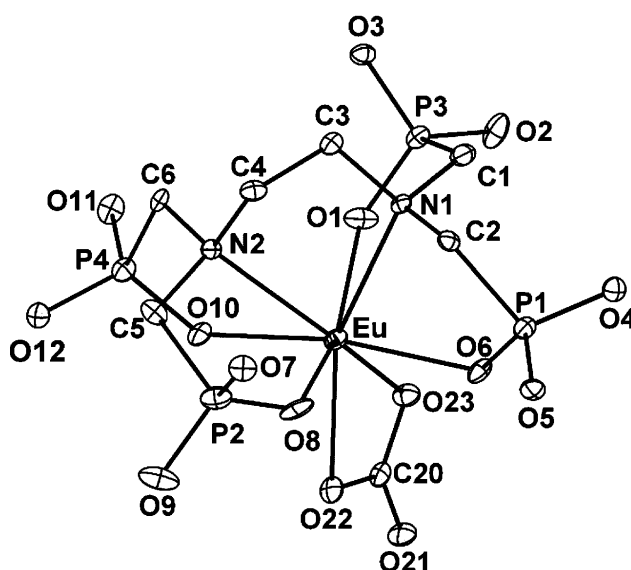


Figure 4. X-ray crystal structure of $[\text{Eu}(\text{EDTMP})(\text{CO}_3)]^{7-}$. Copyright © 2006, Royal Society of Chemistry.

Beyer *et al.* have described the influence of EDTMP levels on the biodistribution of ^{141}Ce , ^{145}Sm , ^{149}Gd , ^{167}Tm and ^{225}Ac .³⁸ It was found that, for liver uptake, there was a strong dependence on the ionic radii of the ligand-free cation in question, with ^{141}Ce and ^{225}Ac displaying the greatest hepatic concentration, whilst the uptake of ^{167}Tm was an order of magnitude less.

^{170}Tm -EDTMP has been proposed as a cost-effective alternative to $^{89}\text{SrCl}_2$ for bone pain palliation.³⁹ ^{170}Tm has a lower beta energy than ^{89}Sr (half-life = 50.5 d), and the accompanying gamma photons can be imaged using scintigraphy studies (Fig. 5). The complex was synthesised in the pH range of 5-8 and was characterised by paper chromatography and paper electrophoreses, with a corresponding radiochemical purity of >95%. Biodistribution studies in rats showed good bone uptake (Fig. 5) with low dosage to soft tissue and vital organs.

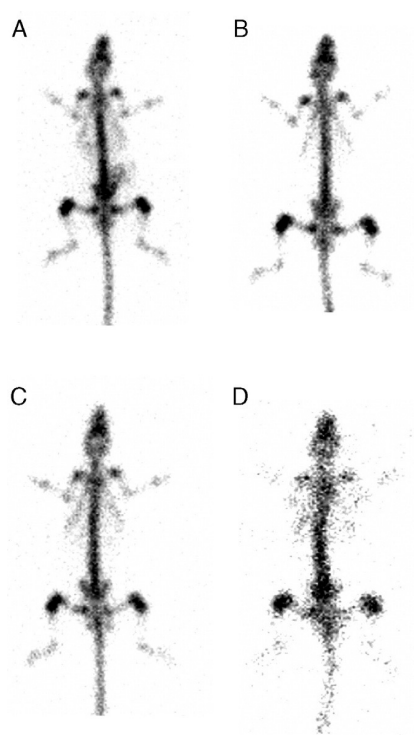


Figure 5. Scintigraphic images of Wistar rats recorded after administration of ^{170}Tm -EDTMP at (A) 3 h, (B) 7 days, (C) 15 days and (D) 60 days. Copyright Das *et al.* Nucl. Med. Biol. 36 (2009) 561-568 (2009 Elsevier Ltd).

^{177}Lu -EDTMP and ^{177}Lu -DOTMP (Fig. 6, discussed later) have been isolated using $^{177}\text{LuCl}_3$.⁴⁰ The long-term storage radiochemical purities were found to be very good with the DOTMP species showing the better resilience; both compounds possess high *in vitro* stabilities. Bone uptake studies on rats showed that the EDTMP complex performed the best, but with higher retention in the liver and kidneys.

Following on from the successful application of EDTMP-based complexes, a large number of structurally related acyclic aminophosphonate ligands (Fig. 2) have been studied. A relatively rare example of ^{175}Yb chemistry has involved the development of complexes with a range of these acyclic polyaminophosphonates (Fig. 2), including EDTMP, PDTMP (propylenediaminetetramethylenephosphonic acid), DTPMP (diethylenetriaminopentamethylenephosphonic acid) and TTHMP (tetraethylenetetraaminohexamethylenephosphonic acid).⁴¹ The complexes were synthesised from $^{175}\text{YbCl}_3$ and were analysed and purified using paper chromatography and paper electrophoresis.

The propylene bridged ligand PDTMP (Fig. 2) has also been complexed with ^{153}Sm .⁴² The complex showed good stability at pH 8.5, but less so at physiological pH where ~13% of radiochemical activity was lost. Biodistribution studies using rats showed some uptake in bone, rapid blood clearance and some uptake in liver (which may be due to the speciation of liberated ^{153}Sm) and kidney.

3-Amino-(1-hydroxypropane-1,1-di-yl)-bisphosphonic acid (Fig. 2) is also known as pamidronic acid (often abbreviated to PMD), and is already used therapeutically (pamidronate therapy) in its own right as a treatment for osteoporosis, Paget's disease, steroid-induced bone loss and certain cancers.⁴³ Its biological half-life is 28.7 h⁴⁴ and it is an effective sequesterer of Ca^{2+} , being able to moderate high Ca^{2+} levels in the body. Closely related ligands such as alendronic and neridronic

acids, are also known (Fig. 2). Early studies have shown a relatively simple synthetic route to these ligands and described the synthesis of the ^{153}Sm complexes.⁴⁵ The results of experimental hydroxyapatite binding showed that ^{153}Sm -alendronate was preferred to the pamidronate and neridronate variants, perhaps due to the interactions of the chain group. From a synthetic perspective recent reports have also shown how to generate the phosphonic esters of these three ligand derivatives.⁴⁶

The ^{166}Ho complex of pamidronic acid has been suggested for bone pain palliation therapy,⁴⁷ wherein good bone uptake was noted after 48 h, although at a level that was not superior to ^{166}Ho -EDTMP. Interestingly, the solid-state X-ray structural properties of Ln(III) complexes (Ln = Eu, Tb, Sm, Nd) of pamidronate were only recently reported⁴⁸ and show 3D open frameworks, which are presumably unlikely to be representative of the solution state speciation relevant to the radiolanthanide work. A recent DFT study also proposed that the pamidronate is likely to act as a tridentate ligand to Sm(III).⁴⁹ The precise speciation and thermodynamic properties of Ln(III) pamidronate (or related) complexes in aqueous solution has not been reported.

Zoledronic acid ((1-hydroxy-2-imidazol-1-yl-phosphonoethyl)phosphonic acid) is a biphosphonic acid (Fig. 2) which is closely related to the pamidronate-like ligands described above. It also has a high affinity for bone and is a known inhibitor of osteoclastic bone resorption. It is chemically robust under physiological conditions, is not biotransformed *in vivo*, and is a well-established therapeutic in its own right.⁵⁰ Zoledronic acid has been radiolabelled with a number of radionuclides including $^{99\text{m}}\text{Tc}$ for bone imaging⁵¹ and ^{14}C in research studies into drug binding.⁵² More recently, the ^{177}Lu complex of zoledronic acid has been isolated in good radiochemical yield and shown good stability in the presence to human serum albumin, although the precise speciation has not been determined. The complex showed good bone uptake in rat

studies, but was not superior to the performance of ^{177}Lu -EDTMP.⁵³ Interestingly, the combined use of zoledronic acid and ^{153}Sm -EDTMP has been investigated in hormone-refractory prostate cancer patients with bone metastases.⁵⁴ In terms of the Ln(III) coordination chemistry, there do not appear to be any specific reports on the structural properties of zoledronate complexes.

The related tetraphosphonate derivative APDDMP (dimethylenephosphonate-1-hydroxy-4-aminopropylidenediphosphonate, Fig. 2) can be conveniently synthesised from pamidronic acid. Both ^{166}Ho and ^{153}Sm complexes of the bone-seeking ligand APDDMP have been isolated and assessed for stability and biodistribution in baboon animal studies.⁵⁵ The studies show that ^{166}Ho -APDDMP has little liver or bone uptake, but that ^{153}Sm -APDDMP does have moderate bone uptake. A key observation from this work is the strong affinity of APDDMP for Ca(II), which can then liberate Ln(III). Interestingly, the modelled speciation for the Ho(III) and Sm(III) species is very different, despite a very small difference in the formation constants of the predominant ML(OH) species ($\log K_{\text{ML}} \sim 18\text{-}19$), and this apparently manifests in very different *in vivo* speciation. The results for ^{153}Sm -APDDMP point to inferior performance compared to ^{153}Sm -EDTMP.

3.1.2. Macrocyclic ligand derivatives

The biomedical applications of macrocyclic ligands are well established and have been summarised elsewhere.⁵⁶ For readers interested in the direct comparison of tetraazamacrocycles bearing methylphosphinic and methylphosphonic acid arms with their aminocarboxylate (*i.e.* acetate) analogues, we highly recommend the review by Lukes *et al.*⁵⁷ Within that overview, the assessment of stability constant data

suggested that for the Gd(III) complexes of a given macrocycle framework, the $\log K_{ML}$ values vary according to phosphonic > acetate > phosphinic derivatives.

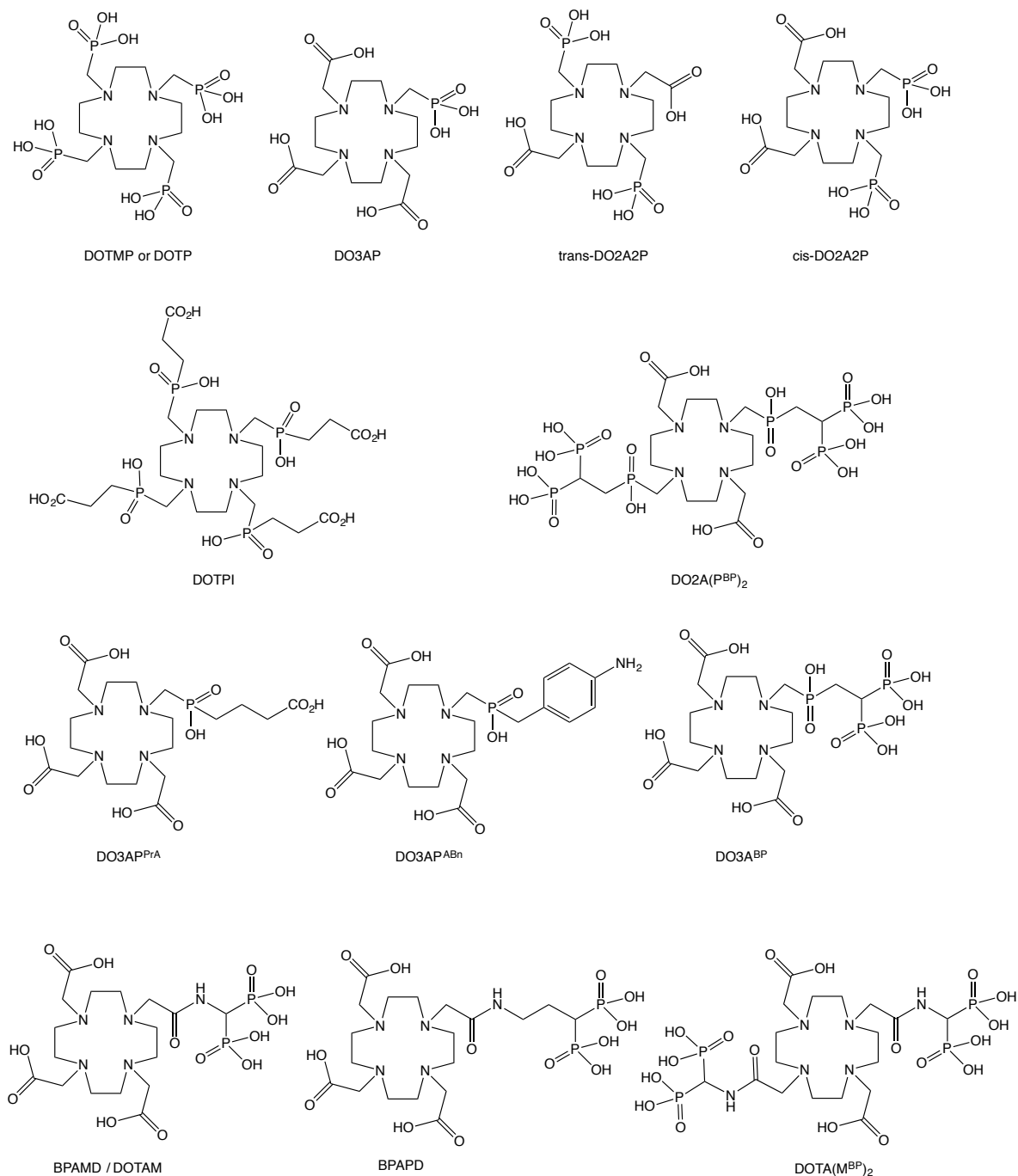


Figure 6. Examples of macrocyclic ligands based on aminophosphonic acids.

The tetraaza macrocyclic framework cyclen has yielded a wide range of phosphonic acid derivatised ligands (Fig. 6). Early work by Sherry and co-workers described the Ln(III) coordination chemistry and characterisation of the classical tetrakisphosphonate ligand DOTMP (also known as DOTP).⁵⁸ Importantly, from a biological and radiopharmaceutical perspective, the $\log K_{ML}$ stability constants for lanthanide ion complexes of DOTMP are in the range of 27.6-29.6 for La(III) to Lu(III).

Both DOTMP (Fig. 6) and its related cyclam cousin, CTMP (also known as TETP, Fig. 7), have been used as ligands for ^{177}Lu , again with a view to future potential as bone pain palliation agents.⁵⁹ The study showed that whilst the DOTMP was efficiently labelled with ^{177}Lu the corresponding CTMP reaction was poorer yielding and required higher, and thus less convenient, reaction temperatures to effect complexation. ^{177}Lu -DOTMP showed selective skeletal uptake, minimal organ uptake and rapid blood clearance in biodistribution studies in rats. ^{141}Ce -DOTMP has been examined as a theranostic agent for metastatic bone tumours, which demonstrated a strong selectivity for bone, with excess activity being excreted renally.⁶⁰

^{177}Lu has also been used to radiolabel macrocyclic bisphosphonates, such as $\text{DOTA}(\text{M}^{\text{BP}})_2$, $\text{DOTA}(\text{P}^{\text{BP}})_2$, DO3AP^{BP} , $\text{DO2A}(\text{P}^{\text{BP}})_2$, BPAPD, and NO2AP^{BP} (Fig. 6) that target bone metastasis for cancer treatment. Binding to hydroxyapatite was measured *in vitro* and all ^{177}Lu complexes showed exclusive accumulation in the skeleton of Wistar rats with very low soft-tissue accumulation.⁶¹ The bisphosphonate complexes of $\text{DOTA}(\text{M}^{\text{BP}})_2$ $\text{DO2A}(\text{P}^{\text{BP}})_2$ showed a slightly higher bone accumulation, but slower blood clearance.

The ligand *trans*-DO2A2P (Fig. 6) has been synthesised and a series of corresponding lanthanide complexes were prepared and their properties investigated

in solution and solid state.⁶² The stabilities of the Ln(III) complexes were intermediate to those of DOTA and DOTP. Of particular interest was the Ce(III) complex, which was more kinetically inert than the analogous Eu(III), Gd(III) or Yb(III) complexes. It was noted that increasing the number of phosphonate donors increased the kinetic inertness of the Ce(III) complex, while conversely, increasing the number of carboxylate donors increased the thermodynamic stability of the Eu(III) complex. In the solid state, ennea-coordinate complexes were observed for Ce(III), Nd(III), Sm(III) while eight coordinate complexes were observed for Eu(III), Tb(III), Dy(III), Er(III), and Yb(III). The radiolabeling of this ligand has also been reported: ¹⁵³Sm and ¹⁶⁶Ho complexes of *trans*-DO2A2P have been prepared (70 °C, pH 8–9).⁶³ These complexes were stable in physiological solutions for up to 48 h, and show low plasmatic protein binding and some *in vitro* hydroxyapatite adsorption, specifically for ¹⁶⁶Ho-*trans*-DO2A2P. Both complexes are stable *in vivo*, have a fast tissue clearance with a rapid excretion from the whole animal body. Bone uptake was greater than for analogous DOTA complexes, but less than half that observed in related DOTP complexes.⁶⁴ The accumulated radioactivity rapidly decreased with time.

The ligand pair of geometric isomers *cis*-DO2A2P and *trans*-DO2A2P (Fig. 6) have been studied with respect to their comparative biological behaviour.⁶⁵ Both isomers were radiolabelled with ¹⁷⁷Lu, for potential applications such as radiotherapy and/or imaging of bone diseases. Biological assays, such as hydroxyapatite binding, *in vitro* stability, and *in vivo* distribution, showed the pair had almost identical biological properties.

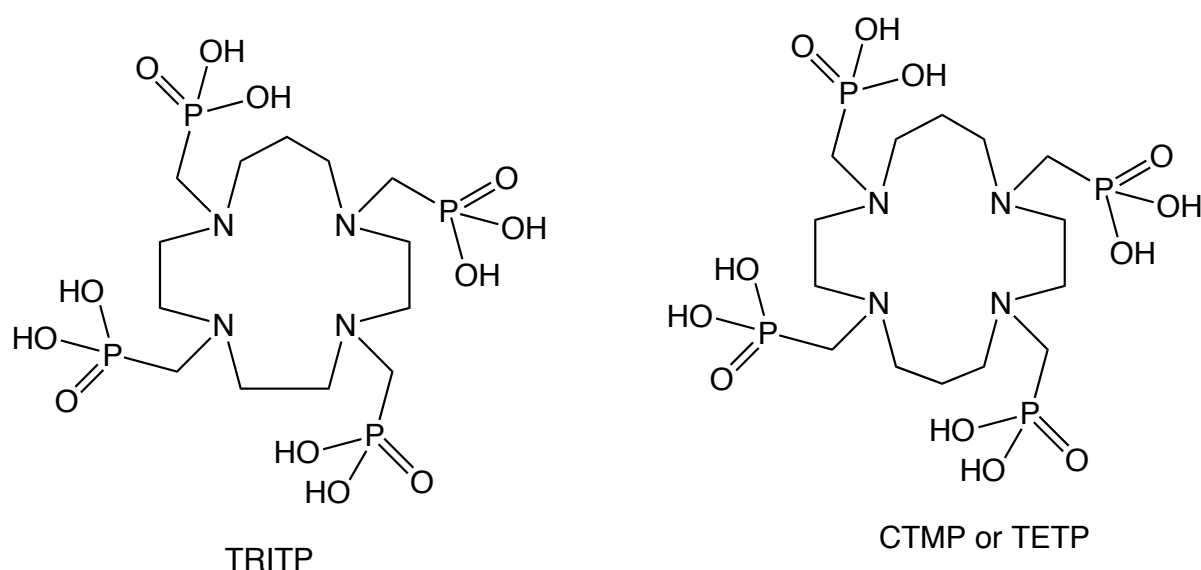


Figure 7. 13- and 14-membered macrocyclic ligands based on aminophosphonic acids.

An assessment of both the ^{153}Sm and ^{166}Ho complexes of 13- and 14-membered azamacrocyclic ligands with phosphonate pendant arms (Fig. 7) has been reported.⁶⁶ The study also included the ligands DOTP, TRITP and TETP (as well as closely related aminocarboxylate derivatives). High radiolabelling efficiencies (>98%) were reported for each ligand and it was noted that the $^{153}\text{Sm}/^{166}\text{Ho}$ -TRITP complexes bound to hydroxyapatite, which manifested in good bone uptake in corresponding biodistribution studies.⁶⁷

In an unrelated study, ^{160}Tb has been used for the physical study of the adsorption of lanthanide complexes to hydroxyapatite;⁶⁷ complexes of the phosphonate ligands DO3A^{BP} and DOTP were studied. Adsorption was found to be very fast for both complexes, with the ^{160}Tb -DO3A^{BP} complex showing a greater affinity for the hydroxyapatite surface than ^{160}Tb -DOTP, presumably due to the availability of the pendant bisphosphonate group.

A large number of DOTA analogues have been synthesised that incorporate monophosphinic acid groups, primarily with a view to their Gd(III) chemistry and MRI applications. For example, DO3AP^{ABn} was described by Hermann and co-workers.⁶⁸ Radiolabelling of DO3AP, DO3AP^{PrA} and DO3AP^{ABn} (Fig. 6) have been described with ¹⁵³Sm and ¹⁶⁶Ho.⁶⁹ The study also included detailed thermodynamic studies which provide the stability constant data for the different Ho(III) and Sm(III) complexes in the series. Interestingly, the data showed log K_{ML} values ca. 24-28, revealing complexes of high stability. All complexes showed low human plasma protein binding and a good biological profile (*i.e.* rapid clearance from the main organs and a high rate of whole body excretion of radioactivity) with the phosphorus substituent imparting little influence upon the key physical and biological properties.

Another class of macrocyclic ligand that has been studied incorporates pyridine donors into the ring. A range of 14-membered, pyridine containing, tetraazamacrocycles (ac₃py14, MeP₂py14 and P₃py14) that incorporate acetic acid or phosphonic acid arms have been reported (Fig. 8).⁷⁰ The stability constants of the Sm(III) and Ho(III) complexes⁷¹ of ac₃py14 are significantly lower (log K_{ML} = 9.78/10.31) than the analogous MeP₂py14 and P₃py14 (log K_{ML} = 17.26/16.84 and 18.87/19.16, respectively) complexes, and notably lower than corresponding DOTA-type species. The ¹⁵³Sm and ¹⁶⁶Ho complexes show considerable bone uptake which has been ascribed to the complexes not being kinetically inert resulting in the *in vivo* metal release. This also results in significant protein binding, high liver and spleen uptake and slow excretion rates.

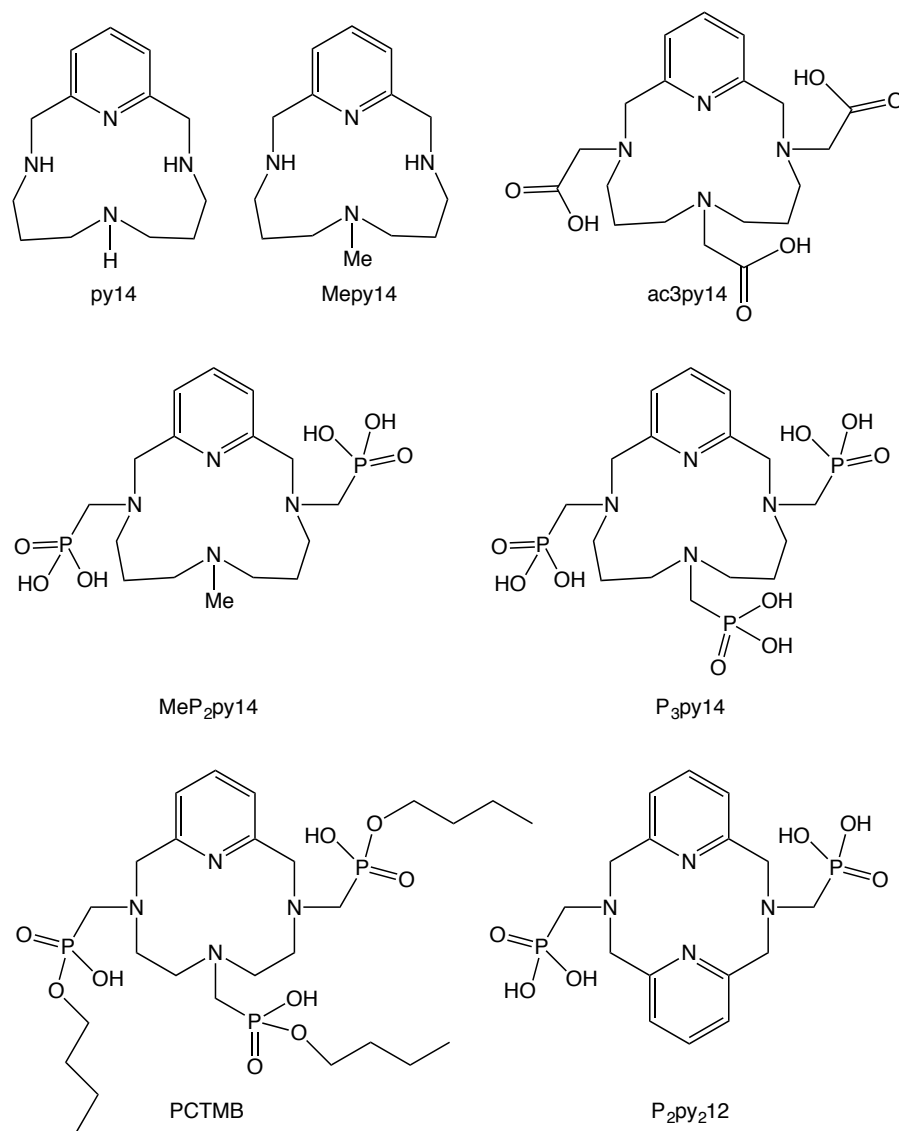


Figure 8. Examples of 12- and 14-membered macrocyclic ligands that incorporate pyridine donors.

12-membered tetraaza macrocycles with integrated pyridine rings are also well known. Two decades ago Bornhop and co-workers pioneered the development of luminescent lanthanide imaging agents based on ligands such as PCTMB and P₂py₂12 (Fig. 8).

The luminescent Tb(III) complexes possess high quantum yields⁷² and supporting studies reported the use of ¹⁵³Sm complexes which showed localisation in bone tissue of rats.⁷³ It is noteworthy that related coordination chemistry with ⁹⁰Y has been reported with PCTMB (Fig. 8).⁷⁴

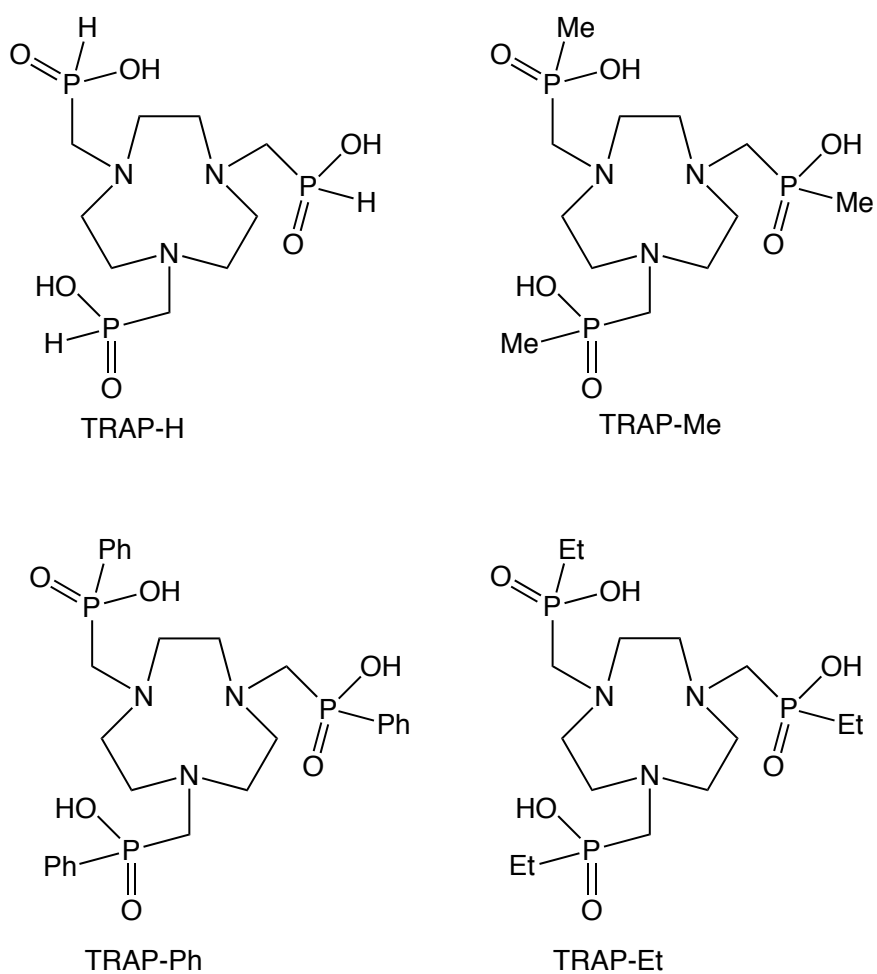


Figure 9. Structures of TRAP ligands (based on the TACN framework).

The re-emergence in the potential use of phosphinic acid functionalised triaza macrocyclic chelators for radiodiagnostics and radiotherapeutics has been recently

reviewed.⁷⁵ In particular, a class of ligand based on 1,4,7-triazacyclononane (TACN) are known as TRAP (1,4,7-triazacyclononane phosphinic acid) ligands (Fig. 9) and were originally developed by Parker and co-workers more than 20 years ago.⁷⁶ The original design of such systems was to address the chelation of ^{67}Ga and ^{111}In based radiopharmaceuticals (Table 1) wherein the phosphinate substituents influenced the overall lipophilicity of the complex and thus biodistribution. After a number of years, interest in TRAP type ligands has increased again with the investigation of ^{68}Ga complexes that show good affinity for bone. Indicative stability constants for Ga(III) complexes of these ligands are in the region of $\log K_{\text{ML}} = 21\text{-}29$. Comparison with Y(III) ($\log K_{\text{ML}} \sim 10$), La(III) ($\log K_{\text{ML}} \sim 7\text{-}11$) and Gd(III) ($\log K_{\text{ML}} = 8\text{-}14$) complexes shows that these ligands result in significantly lower $\log K_{\text{ML}}$ values for the lanthanide series. Unfortunately, these lower stability constants for Ln(III) complexes would seem to preclude their biological and/or clinical application.

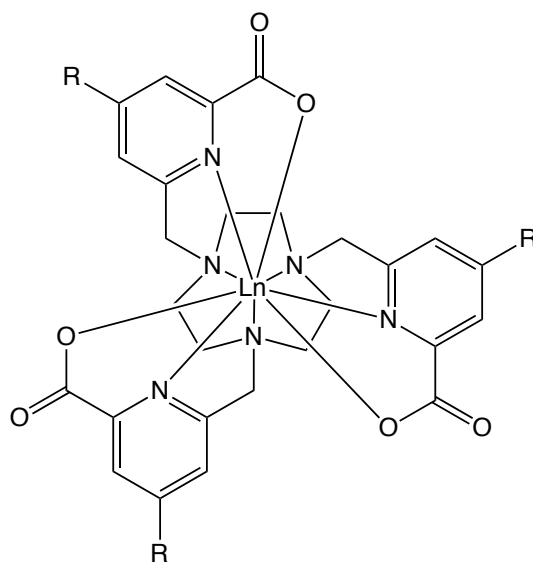


Figure 10. Dipicolinate functionalised TACN ligands for the stabilisation of Ln(III) complexes.

However, more recent progress has shown that stable Ln(III) complexes can be achieved through functionalisation of the TACN framework with dipicolinate arms (Fig. 10).⁷⁷ Such ligands have already been applied to optical biological imaging (fluorescence microscopy) using Sm(III)⁷⁸ and other emissive Ln(III) ions, and therefore clearly represent an interesting option for radiolanthanides through the ease of functionalisation of the peripheral dipicolinate arms. Mazzanti and co-workers have also synthesised a range of picolinate-substituted TACN ligands for Gd(III) and the stability constants of these species range from $\log K_{ML}$ 13.9-19.5.⁷⁹ Of course the radiological robustness of such systems would need to be evaluated.

3.2. Complexes based on (poly)aminocarboxylic acids

EDTA, DTPA and DOTA are the quintessential polyaminocarboxylate ligand frameworks, and their corresponding coordination chemistries have been studied in great detail over a number of decades. In a biological, pharmaceutical and bioimaging context, Ln(III) complexes of DTPA and DOTA (and their derivatives) continue to attract attention. In particular, the applications of DOTA⁸⁰ and peptide-conjugated DOTA⁸¹ derivatives are prevalent.

The $^{144}\text{Ce}/^{144}\text{Pr}$ system has found application as a radiotracer in nutritional science more than 30 years ago, where the elimination of the Ln-EDTA complex in sheep was found to be more rapid than the corresponding ^{51}Cr system.⁸² The complex ^{51}Cr -EDTA was excreted faster in faeces than $^{144}\text{Ce}/^{144}\text{Pr}$ when both were given together as a single injection into the reticulorumen.

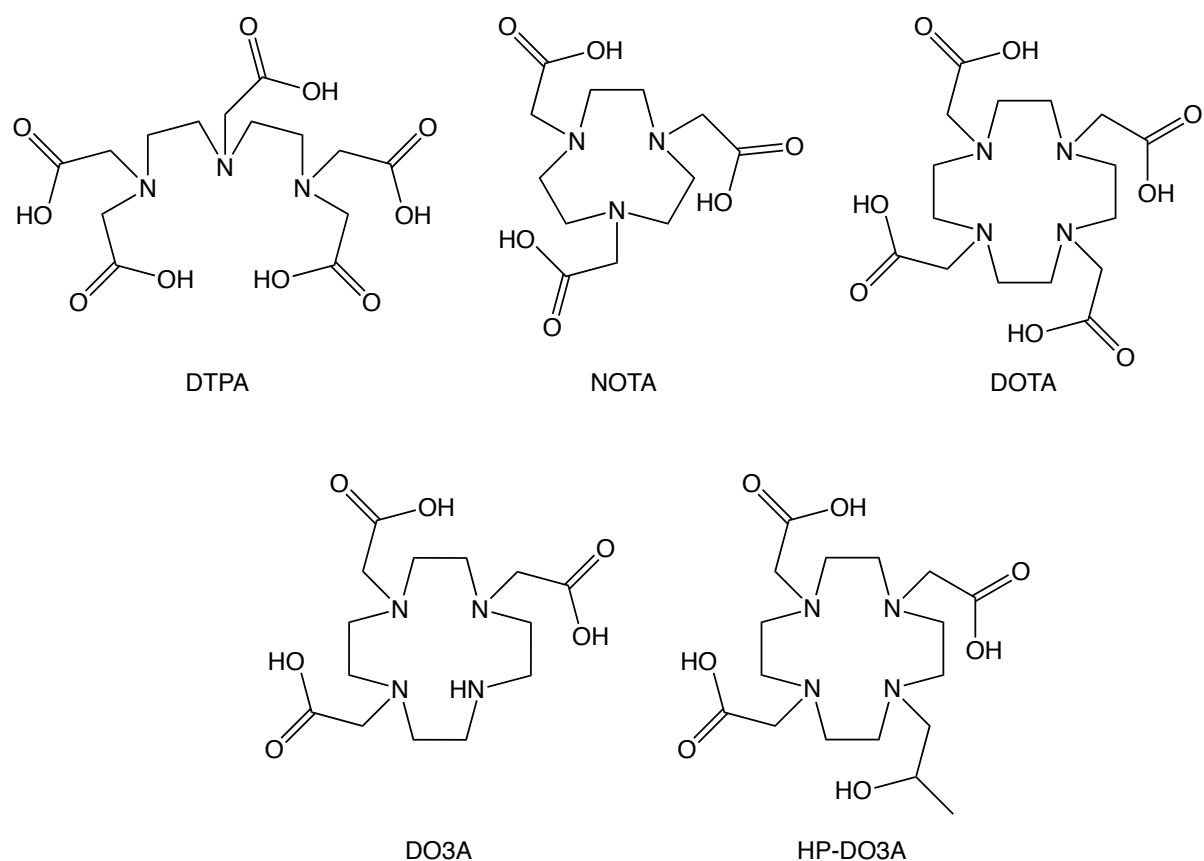


Figure 11. Classical polyaminocarboxylate ligands.

In fundamental studies, Sherry and co-workers previously reported the thermodynamic properties of Ln(III) complexes of common triaza and tetraaza macrocycles, including EDTA, NOTA, DTPA and DOTA (Fig. 11).⁸³ Early studies on related DO3A and HP-DO3A (Fig. 11) have also reported the Ln(III) stability constants for such complexes showing that $\log K_{ML}$ values decrease according to the trend DOTA > HP-DO3A > DO3A.⁸⁴ Table 3 summarises some key stability constant data for a range of relevant Ln(III) complexes based on some of these common ligand frameworks.

Table 3. Stability constant ($\log K_{ML}$) data for selected ligands and relevant Ln(III).

| Ligand | Stability constant ($\log K_{ML}$) | | | | | | |
|--------|--------------------------------------|-------------------|-------------------|-------------------|-------------------|-------------------|-----------------------------------------|
| | Ce(III) | Pr(III) | Sm(III) | Gd(III) | Tb(III) | Ho(III) | Lu(III) |
| EDTA | | 16.4 | 17.1 | 17.3 ^f | 17.9 | 18.6 | 19.8 |
| DTPA | | 21.1 | 22.3 | 22.3 ^f | 22.7 | 22.7 | 22.4 |
| NOTA | 13.2 | 13.3 ^f | 13.8 ^f | 14.5 ^f | 15.1 ^f | 15.2 ^f | 16.0 ^f |
| DO3A | 19.7 | | | 21.0 ^e | | | 23.0, ^a 21.4 ^b |
| DO3AP | | | 28.7 ^c | | | 28.5 ^c | |
| DOTA | 23.4 | 25.5 | 26.1 | 25.3 ^e | 26.2 | 26.1 | 25.5 |
| DOTMP | | 27.4 ^d | 28.1 ^d | 28.8 ^d | 28.9 ^d | 29.2 ^d | 29.6 ^d |
| PCTA | 18.2 | | | 20.4 | | 20.2 | |

^a K. Kumar, *et al.* Pure & Appl. Chem. 65 (1993) 515-520; ^b A. Takacs, *et al.* Inorg. Chem. 53 (2014) 2858-2872; ^c S. Lacerda, *et al.* J. Label Compd. Radiopharm. 53 (2010) 36-43; ^d A.D. Sherry, *et al.* Inorg. Chem. 35 (1996) 4604; ^e K. Kumar, *et al.* Inorg. Chem. 32 (1993) 587-593; ^f W.P. Cacheris, *et al.* Inorg. Chem. 26 (1987) 958-960.

One of the key applications of polydentate aminocarboxylate ligands, such as DTPA and DOTA, has been in the successful development of Gd(III)-based magnetic resonance imaging (MRI) contrast agents, some of which were first approved for clinical use in the 1980s.⁸⁵ Interestingly, this is a branch of research that has exploited ¹⁵³Gd and is focused upon understanding the possible brain deposition of Gd(III) following administration of a contrast agent.⁸⁶ ¹⁵³Gd-labelled DTPA, DOTA and acetate have been studied in mice,⁸⁷ as well as the biodistribution of ¹⁵³Gd labelled analogues of FDA-approved commercial MRI contrast agents, gadopentetate (Gd-DTPA),

gadoterate (Gd-DOTA) and gadodiamide (a diamide derivative of DTPA).⁸⁸ In related work, a ^{153}Gd -labelled complex of HP-DO3A was also obtained, using $^{153}\text{GdCl}_3$ as the source radionuclide.⁸⁹

DO3A and DO2A are well known related ligand scaffolds that allow great flexibility and design potential through functionalisation at the macrocycle unit. Radiolabelled ^{153}Sm species have been reported that use these chelating agents as core units that are functionalised with different glycoconjugates. The specific choice of sugar moiety attached to the ^{153}Sm complex, *via* the macrocycle, resulted in different targeting abilities of ^{153}Sm *in vivo*.⁹⁰

Lanthanide complexes of the pyridine containing 12-membered macrocycle PCTA (3,6,9,15-tetraazabicyclo[9.3.1]pentadeca-1(15),11,13-triene-3,6,9-triacetic acid) have been studied by Sherry and co-workers who reported the stability constant data for a range of Ln(III) species (Table 3), which typically lie in the $\log K_{\text{ML}}$ range 18-20.⁹¹ While these ligands appear more suited to smaller ions such as Ga(III) and In(III), the fast formation kinetics for the Ln(III) species appear attractive from a radiopharmaceutical perspective, and the chelate can be easily functionalized for bioconjugation.⁹²

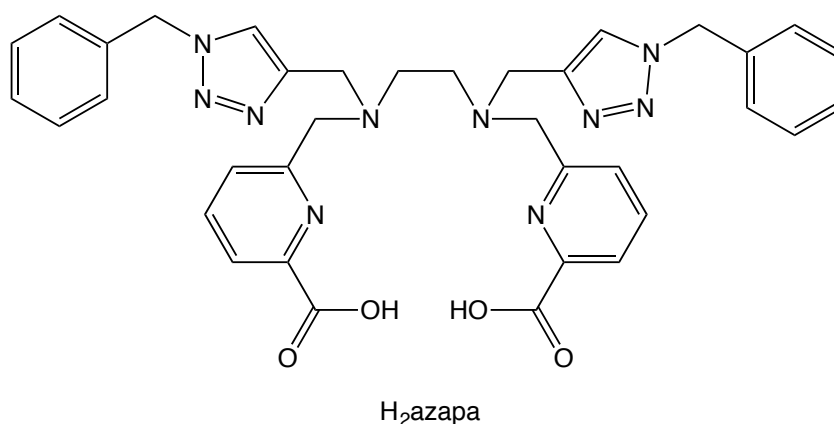


Figure 12. An acyclic ligand suitable for chelating ^{177}Lu .

More recently, Orvig and co-workers have developed a number of novel chelating ligand motifs for the consideration of labelling with radiolanthanides. The potentially octadentate H₄azapa (adopting Orvig's nomenclature), which was synthesised using 'click' chemistry from the alkyne precursor, has shown that radiolabelling is possible with several isotopes, including ¹⁷⁷Lu (Fig. 12).⁹³ The related acyclic poly-chelate H₄octapa class of ligand is discussed later.

3.3. Complexes that incorporate porphyrins

The radiolabelling of porphyrins in nuclear medicine has been reviewed elsewhere,⁹⁴ highlighting the large number of metallo-radionuclides that have been investigated in this context, including ^{99m}Tc, ⁵⁷Co, ⁶⁴Cu, ⁶⁷Ga, ⁶⁸Ga, ¹⁰⁹Pd, ¹¹¹In, ²⁰⁹Pb and ²¹³Bi. The first metalloporphyrins based on lanthanides were synthesised in the 1970s⁹⁵ and were initially investigated as shift reagents in NMR.⁹⁶ However, the coordination chemistry of the radiolanthanides appears to be very rare, and we assume this is because the complexes formed with core porphyrin-type ligands do not have the requisite solubility and/or stability under physiologically relevant conditions. It should be noted that radiolabelling of porphyrins with ⁶⁸Ga requires microwave mediated reaction conditions.⁹⁷ The typical coordination mode of a Ln(III) with porphyrin structures is *via* the four nitrogen atoms of the ring (where the metal ion lies above the plane of the four donors); further stabilisation can be achieved by at least three external donors, particularly if these are tethered to the porphyrin core in some way. Alternatively, 'double-decker' or 'triple-decker' arrangements⁹⁸ of alternating porphyrin / Ln(III) can be formed to satisfy the coordinative requirements of the lanthanide.

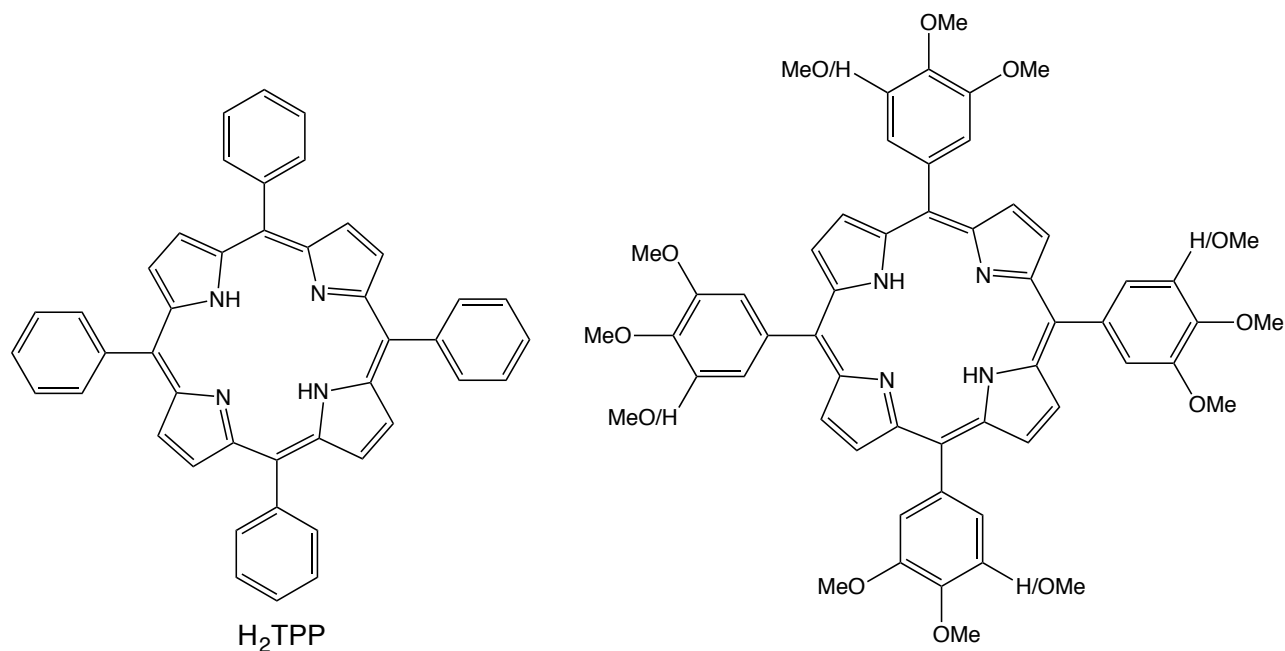


Figure 13. Tetraphenyl porphyrin (TTP) ligands for Ln(III).

A rare report of a directly radiolabelled porphyrin-based chelator⁹⁹ has utilised ¹⁶⁶Ho.¹⁰⁰ The ligands were based around a standard tetraphenyl porphyrin (TPP, Fig. 13) structure with subtle variations in the nature of the peripheral groups to modulate solubility and lipophilicity. The ¹⁴⁰Nd complex of TPP has also been reported,¹⁰¹ possesses high lipophilicity, and apparently showed good radiochemical purity after two days incubation in human serum. The lipophilic character of the complex led to biodistribution in mice into major organs such as liver, lungs and spleen, but also showed significant accumulation in tumours. In both reports, the complexes are assumed to be in a 1:1 stoichiometry with the porphyrin ligand; no spectroscopic or structural data were presented to support these assumptions.

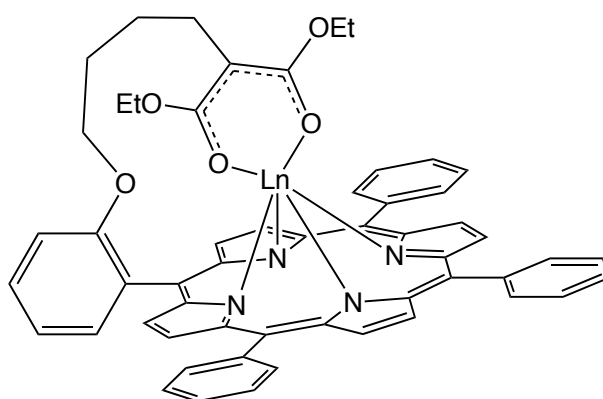


Figure 14. A functionalised tetraphenylporphyrin (TTP) derivative for Ln(III) encapsulation.

Porphyrin-lanthanide complexes that display near-IR luminescent properties has been recently reviewed¹⁰² and therein describes some of the ligand design strategies that are employed to stabilise Ln(III) with porphyrin type ligands. For example, Fig. 14 shows the ligand employed to chelate near-IR emitters Nd(III), Er(III) and Yb(III).¹⁰³ It appears that such strategies have not been employed with radiolanthanides, but may provide useful options in the future design of chelators.

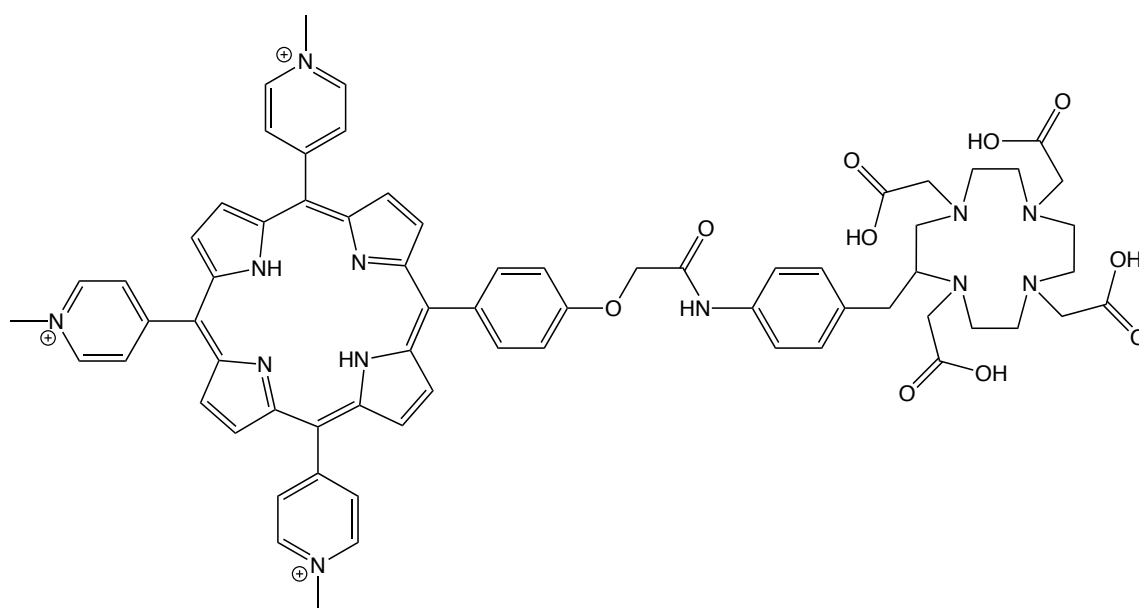


Figure 15. A cationic tetraphenylporphyrin (TTP)-DOTA conjugate.

More commonly, porphyrin groups are often incorporated into complexes and used as targeting vectors, or, to provide dual imaging/therapeutic options for molecule/complex. In this context, the primary advantages in the use of porphyrins are their relatively low toxicity, tumour targeting capability, rapid clearance rates from the body, as well as their application in photodynamic therapy¹⁰⁴ (opening opportunities for dual imaging / therapeutic agents). For example, two cationic porphyrin-DOTA like conjugates (Fig. 15) have been radiolabelled with ^{177}Lu (*via* the DOTA site).¹⁰⁵ Biological evaluation undertaken using mice with fibrosarcoma tumours showed fast tumour localisation of the radiotracer, which was then rapidly cleared and attributed to the hydrophilic, cationic nature of the conjugated ligand.

4. Radiolanthanides labelled with peptides and PRRT (peptide receptor radionuclide therapy)

The synthesis of DOTA-peptide conjugates is a vast subject that is beyond the scope of this review and we recommend the review by Kovacs which deals with this subject in detail.¹⁰⁶ Commonly, it is most convenient for DOTA or DTPA like ligands to be decorated with a reactive functional group, such as an isothiocyanate or an active ester, that allows easy attachment to biomolecules such as peptides. Below we highlight some recent examples that exploit the use of peptide functionalised ligands for radiolanthanides for imaging and therapeutic purposes.

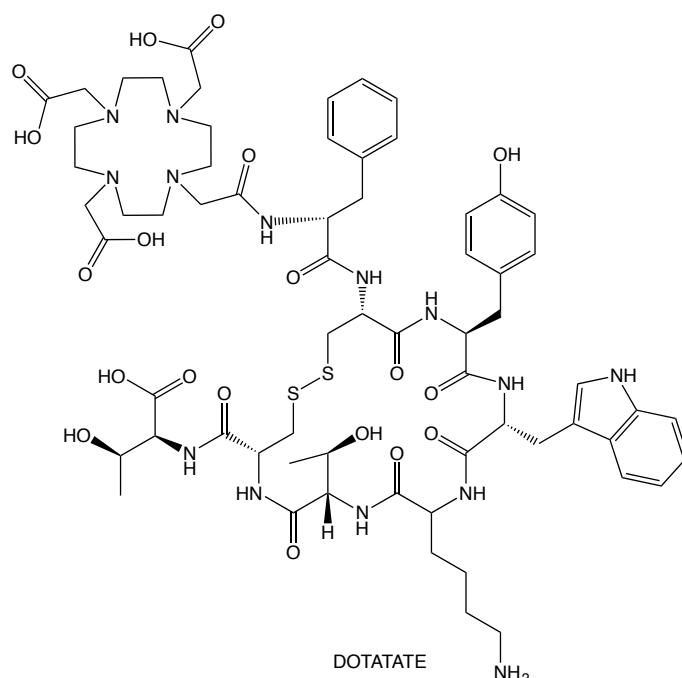


Figure 16. Molecular structure of DOTATATE.

DOTATATE (Fig. 16) is a peptide functionalised derivative of DOTA (also known as DOTATOC, DOTA-octreotate or DOTA-Tyr³-octreotate), and is a ligand that is used in combination with radionuclides for the treatment and diagnosis of cancer. The ⁶⁸Ga complex is used for PET imaging, while the ¹⁷⁷Lu complex of DOTATATE is also available in a small number of research medical centres in the USA and Europe.

A large number of studies have examined ¹⁷⁷Lu radiolabelling of DOTATATE, which includes the effective targeting of radiotherapy in human somatostatin receptor subtype 2 expressed tumours.¹⁰⁷ More recently, the comparative biodistributions and dosimetry profiles of ¹⁷⁷Lu-DOTATATE and ¹⁷⁷Lu-DOTA-anti-bcl-2-PNA-Ty3-octreotate have been reported showing that a more favourable tumour absorbed dose is possible with the PNA peptide variant.¹⁰⁸ Research into the use of ¹⁷⁷Lu-DOTATATE has also included investigating radionuclide therapy in advanced bronchial carcinoids.¹⁰⁹

Amongst the other radiolanthanides, Zhernosekov¹⁹ has reported the synthesis and purification of ¹⁶¹Tb-DOTATATE with the ¹⁶¹Tb obtained from isotopically enriched ¹⁶⁰Gd. The synthesis of ¹⁶¹Tb-DOTATATE was reported using a 1:12 metal:ligand ratio with >99% yield at pH 4.5-5 (100°C, 0.5 h); in comparison, ¹⁷⁷Lu may be more efficiently used at a 1:4 ratio. In plasma, the ¹⁶¹Tb-DOTATATE complex showed the same stability as the ¹⁷⁷Lu analogue. Also reported, is the use of ¹⁵⁵Tb in the formation of complexes of DOTATATE. SPECT imaging was utilised for preclinical evaluation.¹¹⁰

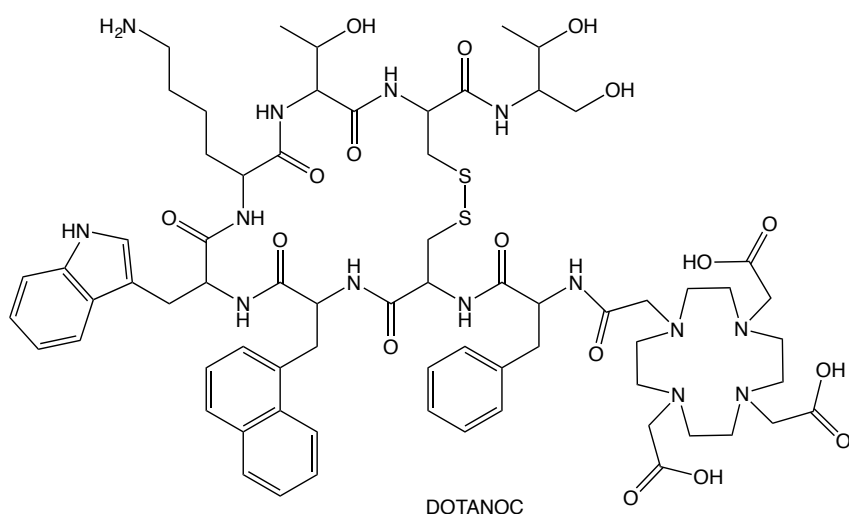


Figure 17. Molecular structure of DOTANOC.

DOTANOC (Fig. 17) is a DOTA peptide conjugate of the somatostatin analogue 1-Nal3-octreotide (NOC). NOC has a high affinity for somastatin receptor types 2, 3 and 5, which are known to be prevalent on neuroendocrine tumours and their metastases (normal tissue shows a low level of receptor coverage). Whilst the ⁶⁸Ga complex of DOTANOC is routinely used for PET imaging of neuroendocrine tumours, a number of radiolanthanides have also been investigated. ¹⁷⁷Lu-DOTANOC is the most widely studied, including patient studies¹¹¹ and a detailed overview of this agent is available elsewhere.²⁴

Much more recently, ^{152}Tb has been complexed with DOTANOC and directly employed for PET scans on AR42J tumour-bearing mice.¹¹² ^{152}Tb was produced by proton-induced spallation of tantalum targets, with separation using cation exchange chromatography. Biodistribution studies (Fig. 18) revealed that injection of the radiotracer using small amounts of peptide resulted in the best tumour-to-kidney ratio. In other studies, the DOTANOC complex of $^{149}\text{Tb}^{113}$ has been reported and its properties evaluated.

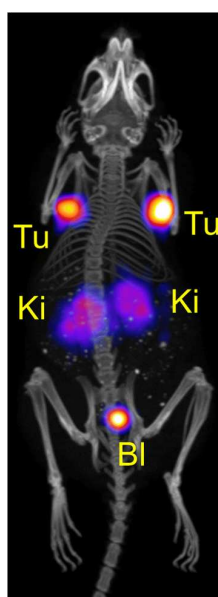


Figure 18. PET/CT image shown as maximal intensity projection of an AR42J tumor-bearing mouse 2 h after injection of ^{152}Tb -DOTANOC (3.4 MBq; 0.34 nmol DOTANOC). Copyright Müller *et al.* *EJNMMI Research* 6 (2016) 35. © 2017 BioMed Central Ltd.

Gastrin-releasing peptide receptors are overexpressed in a number of human cancers and can be targeted using bombesin derivatives of radiopharmaceuticals. The bombesin antagonist peptide sequence (Gln-Trp-Ala-Val-N-methyl-Gly-His-Statine-Leu-NH₂) can be conjugated with a DOTA chelate to give DOTA-sBBNA (Fig. 19) which has been radiolabelled with ¹⁷⁷Lu.¹¹⁴ Resultant biodistribution studies showed high accumulation and retention within tumours and an agent that was rapidly cleared from the blood pool. Earlier work had already reported ¹⁴⁹Pm with DOTA bombesin analogues and showed very similar *in vivo* characteristics to the related ¹⁵³Sm and ¹⁷⁷Lu complexes.¹¹⁵

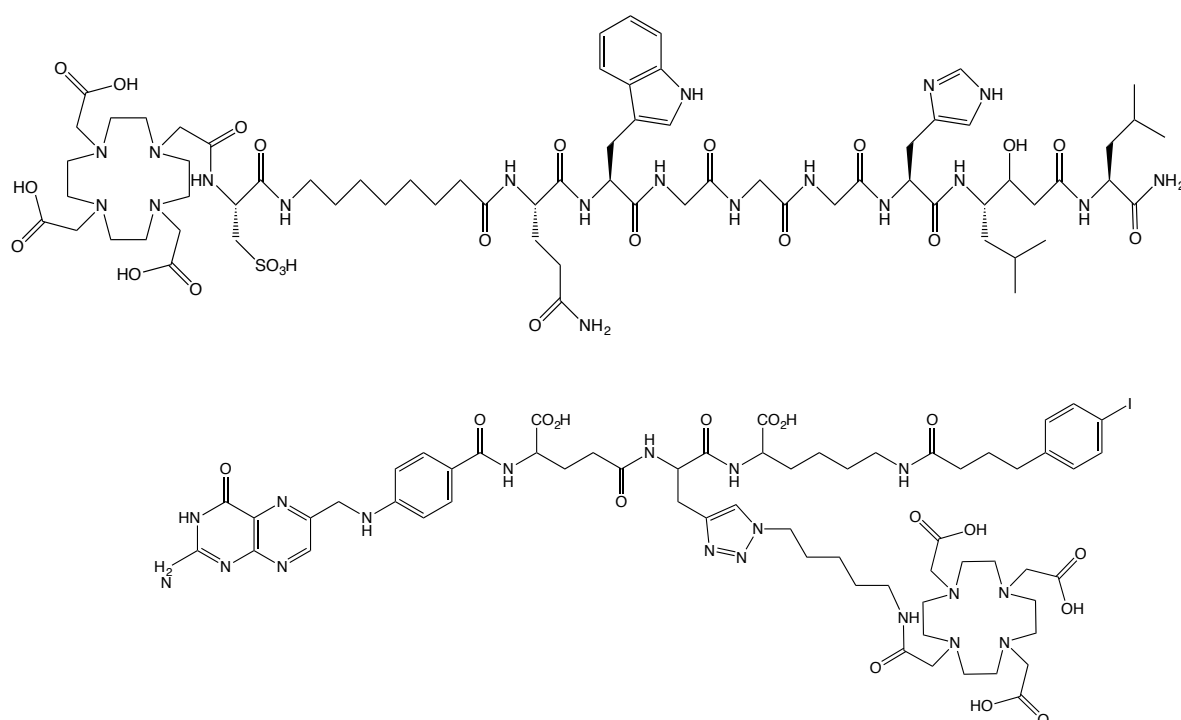


Figure 19. Molecular structures of DOTA-sBBNA (top) and a folate-conjugated DOTA chelate (bottom).

More recently, Muller and van der Meulen reported the use of a DOTA chelate in the preparation of radioactive Tb(III) conjugates.¹¹⁶ They utilised ^{149}Tb , ^{152}Tb and ^{155}Tb isotopes from the ISOLDE facility at CERN,¹¹⁷ as well as ^{161}Tb through neutron irradiation of ^{160}Gd . Folate DOTA conjugates (Fig. 19) of all isotopes were prepared, with the metal being coordinated to a DOTA-like core; the folate is attached *via* a triazole unit and an amide linkage to a DOTA carboxylate group. ^{161}Tb complexes were prepared by standard procedures with the combination of ligand and metal (95°C, pH 4.5). However, complexes of the other isotopes were formed directly in the chromatography elution in an effort to minimize loss of activity. The work demonstrated the potential of α and β therapy by ^{149}Tb and ^{161}Tb , as well as the PET and SPECT imaging capability of ^{152}Tb , ^{155}Tb and ^{161}Tb . It was proposed that this quartet of isotopes offers potential users chemically/biologically identical species for multiple applications.

The melanin-binding decapeptide 4B4 has also been attached to a DO3A chelate and radiolabeled with ^{177}Lu , ^{166}Ho and ^{153}Sm .¹¹⁸ Stability tests in serum and hydroxyapatite assays showed that the ^{177}Lu complex was most stable. However, *in vivo* the ^{177}Lu complex did not display the desired tumour uptake, but rather localized in kidneys.

5. Complexes for radioimmunotherapy applications

The development of ligand-antibody conjugates for radiolabelling is well known,¹¹⁹ and a modern detailed protocol based on the bacterial siderophore Deferoxamine (desferrioxamine) for the conjugation of ^{89}Zr to antibodies *via* a diisothiocyanate phenylene linker has been described.¹²⁰ It is important to note that both the antibody pharmacokinetic (t_p) and tracer radioactive half-lives (t_r) must be taken into

consideration when choosing a tracer isotope. The effective half-life (t_e) is given by $1/t_e = 1/t_r + 1/t_p$ and for those antibodies with long pharmacokinetic half-lives, long lived isotopes with comparable decay parameters should be considered.

Again, the DTPA and DOTA frameworks have been some of the most popular chelators of choice when considering conjugation with biological molecules/vectors. Typically, ligands are adorned with a reactive functional group, such as an isothiocyanate, that allows facile attachment to biomolecules such as monoclonal antibodies.⁷⁶ Examples of this approach have mainly focused on using ^{90}Y and ^{177}Lu radiolabelled bioconjugates, and is covered elsewhere in the literature. Below we highlight some recent examples, as well as detailing other radiolanthanides that have been used in this context.

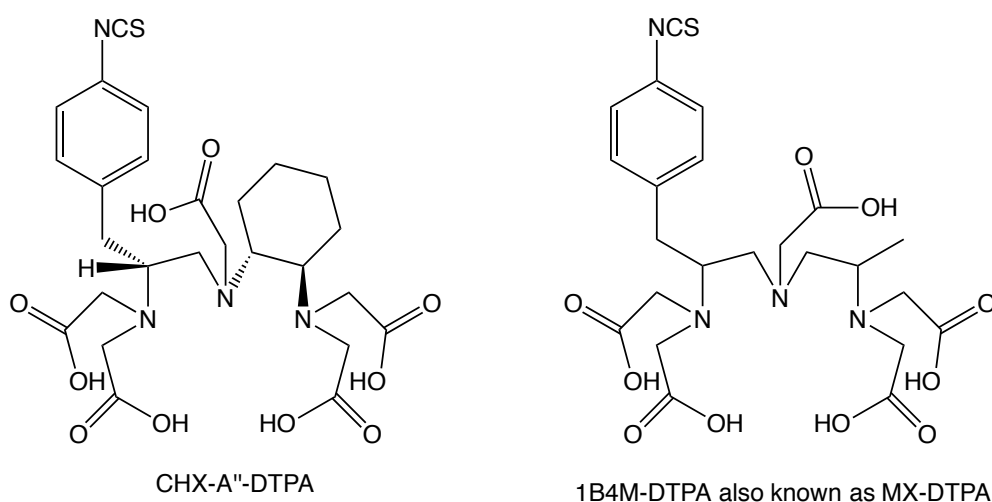


Figure 20. Molecular structures of CHX-A''-DTPA and MX-DTPA.

The DTPA derivative CHX-A''-DTPA (Fig. 20) is a common choice for bioconjugation and recent studies have examined its conjugation with bevacizumab, a humanised

monoclonal antibody to target vascular endothelial growth factor (VEGF) which is secreted by stromal or cancer cells.¹²¹ Radiolabelling with ^{177}Lu has been reported for this conjugate and *in vitro* cell binding studies showed good uptake by VEGF expressing tumour cells. The closely related bifunctional chelate MX-DTPA (Fig. 20) was also an early choice of ligand for labelling the monoclonal antibody K-1-21 with ^{153}Sm .¹²²

Rituximab (anti-CD20) is a specific chimeric monoclonal antibody directed against CD20 surface antigens on B lymphocytes and is used to treat CD-20 positive Non-Hodgkin's Lymphomas.¹²³ Its combination with radionuclides is well known, with two FDA-approved radiopharmaceuticals. While the ^{90}Y (trademarked as Zevalin) is well known, the ^{177}Lu analogue is less understood and the first report of a ^{177}Lu -DOTA conjugate of rituximab dates from 2009.¹²⁴ A more rapid and reliable radiolabelling method with ^{177}Lu has been subsequently reported.¹²⁵ DTPA conjugates with rituximab are also well known and have been radiolabelled with a range of radionuclides including $^{99\text{m}}\text{Tc}$ ¹²⁶ and ^{67}Ga .¹²⁷ Research on the ^{177}Lu -CHX-A"-DTPA-rituximab is well developed and animal studies have shown promising tumour uptake and targeting.¹²⁸ ^{153}Sm -DTPA-rituximab has also been reported and was used to obtain SPECT images on rats¹²⁹ and Beyer *et al.* have described the synthesis and use of ^{149}Tb -CHX-A"-DTPA complexes in the formation of conjugates with the antibody rituximab.¹³⁰

Thompson *et al.* have recently examined the CHX-A"-DTPA conjugates of the melanoma targeting 6D2 antibody in an attempt to correlate isotope half-lives and efficacy for the high energy β -emission of ^{166}Ho and ^{90}Y .¹³¹ The study concluded that the longer lived ^{90}Y system was toxic in the murine model used and that the ^{166}Ho system was more effective as a result of a match between the serum half-life of the

antibody and the physical (decay) half-life of the radiolanthanide. In much more recent studies, the ^{177}Lu complexes of CHX-A"-DTPA have been compared with either conjugated rituximab or huRFB4 (a novel humanised anti-CD22 monoclonal antibody). The resultant studies revealed that tumour growth inhibition was improved with the huRFB4 derivative and further enhanced when combined with unlabelled rituximab.¹³²

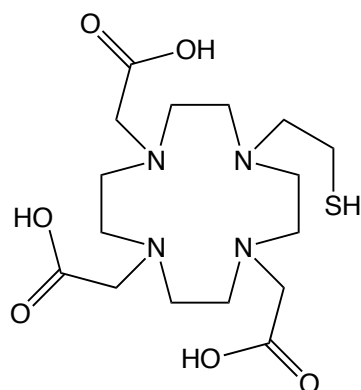


Figure 21. Molecular structure of a thiol functionalised DO3A ligand.

More recently, a thiol functionalised DO3A-type ligand (Fig. 21) has been reported for the coordination of ^{153}Sm and ^{166}Ho with an aim of further bioconjugation *via* the thiol terminus.¹³³ The resultant Ln(III) complexes possessed $\log K_{\text{ML}}$ of 21.0-22.0, and spectroscopic studies showed that the pendant thiol does not coordinate to the Ln(III), even in its deprotonated form. In physiologically modelled medium the ^{166}Ho did not demonstrate sufficient stability, and only the ^{153}Sm complex was assessed for *in vivo* biodistribution studies.

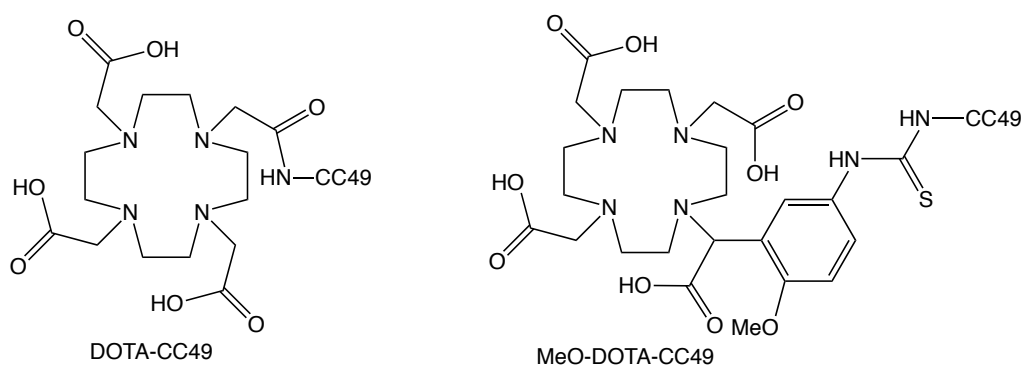


Figure 22. Molecular structures of CC49 conjugates of DOTA-like chelates.

Lewis and co-workers have prepared complex conjugates of various radiolanthanides, including ^{149}Pm , ^{166}Ho and ^{177}Lu (from the University of Missouri Research Reactor), with the CC49 monoclonal antibody as potential agents in radioimmunotherapy.¹³⁴ The CC49 antibody reacts with the tumour-associated glycoprotein-72 (TAG-72) expressed in 85% of human adenocarcinomas (e.g. colon, breast, pancreatic, ovarian, prostate, non-small cell lung and gastric). Two closely related ligand systems were utilised, namely DOTA-CC49 and MeO-DOTA-CC49 (Fig. 22) where the active ester of DOTA was coupled to the antibody to give DOTA-CC49, while an isothiocyanate containing DOTA ligand was coupled to CC49 to give MeO-DOTA-CC49. ^{149}Pm has a half-life (53.1 h) intermediate to ^{166}Ho (26.9 h) and ^{177}Lu (159.6 h) and yields a DOTA complex with a slightly lower stability constant ($\log K_{\text{ML}} = 22.9$ vs 26.1 (Ho) and 25.5 (Lu)), though this is unlikely to cause significant differences in their application. *In vivo* stability was estimated via a hydroxyapatite model¹³⁵ and suggested >92% stability for 168h @ 37°C for all three complexes, although *in vivo* studies showed less than 5% uptake by the bones. Results showed that the MeO-DOTA-CC49 variant offered superior conjugate stability with ^{177}Lu , while in *in vitro* serum studies the ^{177}Lu were

more stable than ^{149}Pm and ^{166}Ho . *In vivo* studies revealed MeO-DOTA-CC49 gave maximal uptake for ^{149}Pm at two half-lives, for ^{166}Ho at four half-lives and one half-life for ^{177}Lu , and thus it was found that the therapeutic efficacies were of the order $^{177}\text{Lu} > ^{149}\text{Pm} > ^{166}\text{Ho}$. Lewis *et al.* extended this work to compare these pre-assembled reagents to a pre-targeting approach of first administering Ln-DOTA-biotin, followed by the later injection of a CC-49-streptavidin fusion protein. Further studies identified the ^{177}Lu species as the most promising for future evaluation in toxicity and multiple dose therapy studies.¹³⁶

Other DOTA conjugated systems include those that have been functionalised with the non-peptide vitronectin receptor antagonist TA138.¹³⁷ Radiolabelling with ^{177}Lu was best achieved using anaerobic formulation conditions that minimised radiolytic degradation of the conjugate. The ^{177}Lu radiolabelled form of the murine 7E11 monoclonal antibody has also been reported, using DOTA as the chelator, as a targeted prostate-specific agent.¹³⁸

^{155}Tb complexes of DOTA-MD (minigastrin analogue: peptide sequence, H-Leu-Glu-Glu-Glu-Glu-Ala-Tyr-Gly-Trp-Met-Asp-Phe-NH), chCE7 (a glycosylated monoclonal anti-L1-CAM antibody) and cm09 (albumin binding entity) derivatives have been evaluated for SPECT imaging in tumour-bearing mice. The chCE7 sequence was conjugated with CHX-A"-DTPA, but no details were given of the method of conjugation for the minigastrin in the ^{155}Tb -DOTA-MD complex. The long physical half-life of ^{155}Tb was found to be a good match to the long biological half-lives of the complexes. The corresponding ^{177}Lu -DOTA-chCE7¹³⁹ and ^{177}Lu -DOTA-cm09¹⁴⁰ species are also known, the latter being the first folic acid targeted radiolanthanide.

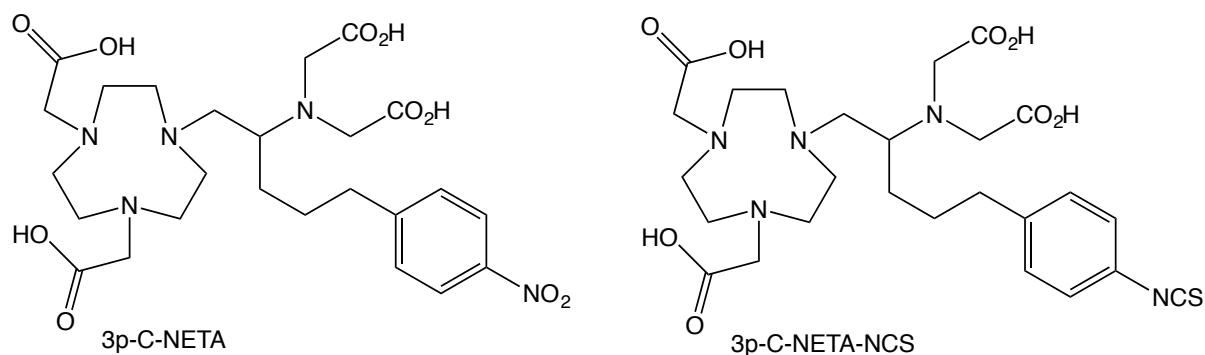


Figure 23. Molecular structures of conjugatable NETA ligands.

Bifunctional NETA (Fig. 23) derivatives (3p-C-NETA),¹⁴¹ that are closely related to the parent NOTA chelate, can be synthesised using a convenient ring opening of an aziridinium ion and have been shown to form stable ¹⁷⁷Lu complexes *via* radiolabelling under physiologically compatible conditions.¹⁴² The complex showed good *in vitro* stability in serum and is postulated as an alternative to DOTA and DTPA derivatives. Further work has described the high yielding synthesis of the isothiocyanate analogue (3p-C-NETA-NCS) which allows facile coupling to trastuzumab (a tumour targeting antibody). ¹⁷⁷Lu-3p-C-NETA-trastuzumab was evaluated *in vivo* and demonstrated a high tumour-to-blood ratio.¹⁴³

Nimotuzumab (h-R3) is a humanised monoclonal antibody and can be conjugated with chelates for radiopharmaceuticals. It binds to the epidermal growth factor receptor, which is often overexpressed in cancer cells. In studies on conjugated chelates DTPA and DOTA it was shown, not unsurprisingly, that ^{177}Lu -DTPA-h-R3

displayed poorer *in vivo* stability when compared to the DOTA analogue, which also demonstrated good tumour specificity and uptake.¹⁴⁴

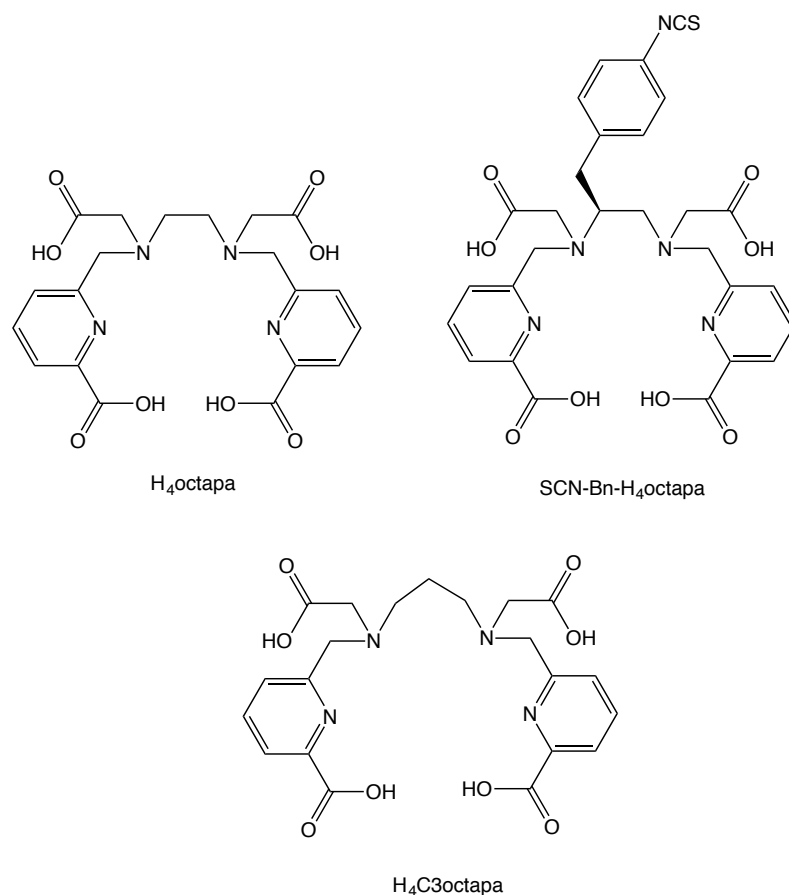


Figure 24. Molecular structures of Orvig's acyclic octapa-type ligands.

Orvig and co-workers recently developed a new class of acyclic chelate (Fig. 24) system ($H_4octapa$) that can be conjugated to the HER2/neu-targeting antibody trastuzumab. One of the octapa systems studied was labelled with ^{177}Lu ; potentiometric titrations showed that the $Lu(III)$ complex of $H_4octapa$ possessed a $\log K_{ML}$ of ~ 20 , whilst NMR studies showed little fluxional conformational behaviour at ambient temperatures.¹⁴⁵ The octapa chelates show some radiolabelling advantages over analogous DOTA conjugates, as well as improved *in vivo* biodistribution profiles and SPECT imaging results when compared to the ^{177}Lu -DOTA-trastuzumab. The

same group has expanded the octapa ligand motif to include a propyl (rather than ethyl) backbone ($\text{H}_4\text{C3octapa}$, Fig. 24), which resulted in a reduced stability constant for the Lu(III) complex and poorer serum stability for the ^{177}Lu analogue.¹⁴⁶

6. Radiolanthanides linked to, or incorporated into, nanostructures and nanoparticles

Radiolabelled nanoparticles or nanomaterials have emerged as a very promising approach for diagnostic applications.¹⁴⁷ Although a wide range of nanoparticle platforms are potentially available for the design of radiolabelled agents, we highlight some examples below that show that demonstrate the breadth of approach with radiolanthanides.

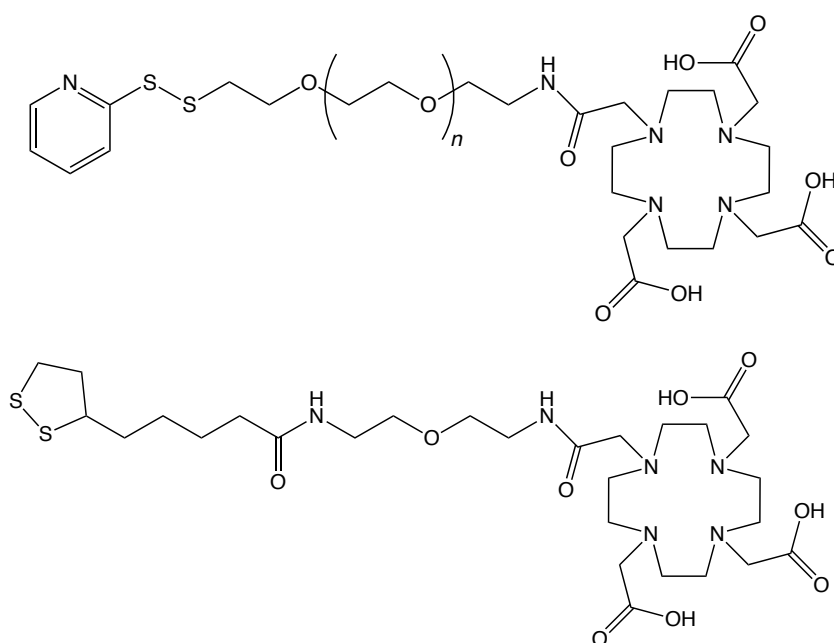


Figure 25. Disulfide functionalised DOTA type ligands for the surface functionalisation of gold nanoparticles (GNPs).

^{177}Lu labelled gold nanoparticles (GNPs) have been developed by covalently linking DOTA-type chelates (Fig. 25) to the surface of GNPs, which have been additionally PEG-ylated for improved solubility.¹⁴⁸ Such systems have been investigated as 'radiation nanomedicines' in the context of EGFR-positive breast cancer, and as injectable brachytherapy for neoadjuvant treatment of locally advanced breast cancer.¹⁴⁹

PEG-labelled GNPs (represented in cartoon form in Fig. 26) have been labelled by ^{177}Lu -DOTA-type complexes to allow a study into the stability, elimination and biodistribution of such conjugates as a function of the nature of the thiol attachment (mono-, di- and multi-thiol attachment at the GNP surface). Studies on athymic mice showed that the multi-thiol attachment at GNP gave the greatest stability *in vivo* and the lowest liver uptake of ^{177}Lu and it is this system that is proposed as a radiation treatment for breast cancer.¹⁵⁰

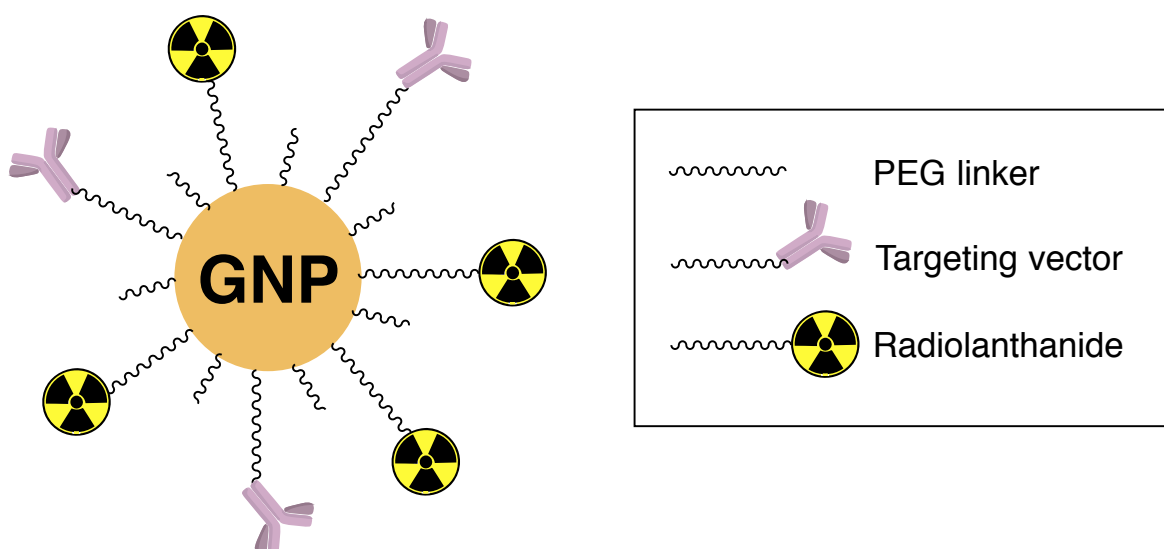


Figure 26. Cartoon representation of a GNP co-functionalised with a radiolanthanide chelate and a targeting vector (such as an antibody).

Shanehsazzadeh *et al.* have described the conjugation of DTPA to a superparamagnetic iron oxide nanoparticle (SPION).¹⁵¹ The complexation of a

radiolanthanide to these ligands will yield potential dual mode imaging agents (SPIONs are known as T_2 MRI contrast agents). Using commercially obtained SPIONs, with an amino functionalised dextran stabiliser coating, DTPA bis-anhydride was reacted with the terminal amine to give a surface-attached pendant DTPA-monoamide ligand. The implied ratio was two ligands to each SPION, though no data was advanced to show this was the case. The ligand was complexed with ^{177}Lu (90 MBq), though the amount of SPION used to complex the ion was not reported. Magnetic separation was used to conveniently isolate the complex (and un-complexed SPION) and chromatography was used to determine the ratio of complex to free Lu(III) ion. It seems probable that a vast excess of SPION-DTPA was used, meaning that the isolated $^{177}\text{Lu(III)}$ species is largely un-complexed ligand that is not readily separated from the complex. *In vivo* studies suggest that the SPION causes fast clearance of the agent from most tissue, with a significant loading in the reticuloendothelial system (liver and spleen).

^{177}Lu -DOTATATE complexes have been encapsulated within PEG-coated PLGA (polylactic-co-glycolic acid) nanospheres,¹⁵² which are a form of biodegradable polymer successfully developed for biomedical applications.¹⁵³ ^{177}Lu -DOTATATE was incubated in the presence of the PLGA nanoparticles to give encapsulation efficiencies of 58-77% based on the activity of the resultant supernatant. The relatively large (ca. 300 nm) spherical particles were co-functionalised with anti- β -hCG antibodies with the aim of enhancing tumour targeting and reducing radiation damage to the kidneys of Wistar rats.¹⁵⁴

EDTMP-doped hydroxyapatite nanoparticles have been reported as a possible means of a new carrier system for radiotherapy.¹⁵⁵ The hydroxyapatite was formulated in the presence of the EDTMP, which then provides the potential chelation site for the

lanthanide although, to the best of our knowledge, the ^{153}Sm has not yet been reported. In related work, EDTMP-capped $\text{NaLuF}_4\text{:Yb,Tm},^{153}\text{Sm}$ upconverting nanoparticles have been proposed as blood pool imaging agents.¹⁵⁶ The nanoparticles show good adhesion to red blood cells and no toxicity at a dose of 100mg/kg in mice. These systems couple useful luminescence properties with SPECT imaging capability (Fig. 27).

Ho(III) has been used as the lanthanide component in the synthesis of iron garnet, which was then spun into polyacrylonitrile bandages.¹⁵⁷ The bandages were then neutron activated to give ^{166}Ho containing bandages. These nanocomposites of ^{166}Ho have been proposed as a feasible avenue for the treatment of skin cancer.

^{177}Lu labelled cerasome particles, that also encapsulates indocyanine green (a FDA approved near-IR fluorescent agent for clinical applications), can be developed from sol gel and self-assembly processes. The ^{177}Lu chelate was a PEG-linked distearoyl terminated DOTA species, and the resultant cerasome was postulated as a dual imaging and phototherapeutic platform for cancer cells.¹⁵⁸

In a separate study, Simonelli *et al.* examined the cytotoxicity of $^{141}\text{Ce-CeO}_2$ nanoparticles on mouse fibroblast Balb/3T3 cells.¹⁵⁹ Multifunctional particles based on radiolabeled (^{141}Ce , ^{111}In and ^{65}Zn) cerium oxide particles have also been described and applied to *in vivo* imaging of nude mice. The surface coating of the CeO_2 can be modified to modulate the physiological and pharmacokinetic properties of nanoparticles.¹⁶⁰

Another approach to the development of radiolabelled particles has investigated the use of ^{177}Lu loaded core-crosslinked polymeric micelles that can be prepared with a DTPA-type chelator.¹⁶¹ This species was investigated in a

combination therapy approach with cyclopamine-loaded liquid-lipid particles in both breast and pancreatic cancer models.

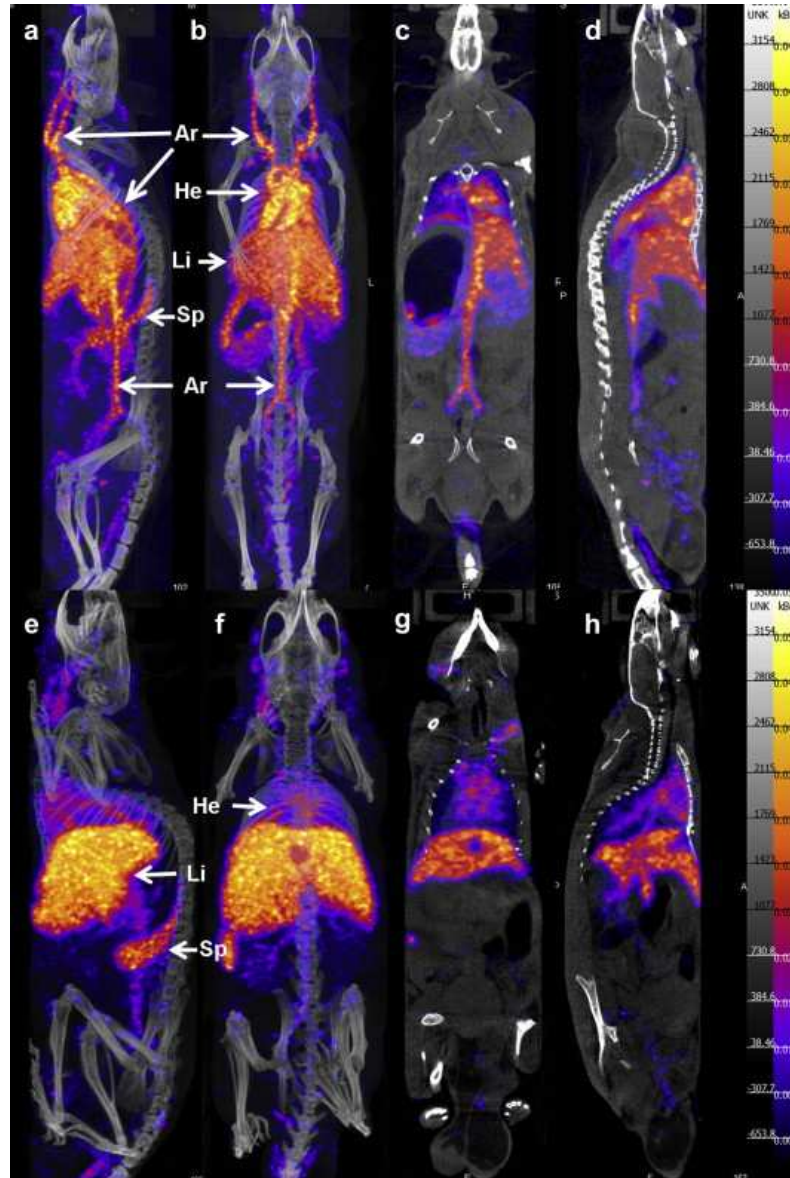


Figure 27. SPECT/CT imaging *in vivo* of mouse after intravenous injection of EDTMP-coated nanoparticle: ^{153}Sm at different time points and different sections. The upper line: (a–b) 3D reconstruction at the different angles of rotation and (c) their coronal plane and (d) sagittal plane of mouse with injection of EDTMP-coated nanoparticle: ^{153}Sm at 0.5 h. The lower line: (e–f) 3D reconstruction of mouse at the different angles of rotation, and (g) their coronal plane and (h) sagittal plane with injection of EDTMP-coated nanoparticle: ^{153}Sm at 1 h. (Ar: Artery, He: Heart, Li: Liver, Sp: Spleen). Copyright Peng *et al.* Biomaterials 34 (2013) 9535-9544 (2013 Elsevier Ltd).

Fe_3O_4 nanoparticles have been investigated for their utility to carry radiolanthanides for the treatment of arthritis. Radiolanthanide loading of the nanoparticles was achieved by replacement of surface Na^+ ions with trivalent ^{153}Sm , ^{166}Ho , ^{169}Er and ^{177}Lu .¹⁶² The materials showed good stability *in vitro* and retained >70% radiochemical purity after 48 h storage in the presence of competing DTPA. This is an interesting, and perhaps surprising observation given the known $\log K_{\text{ML}}$ data for Ln-DTPA complexes (see Table 3).

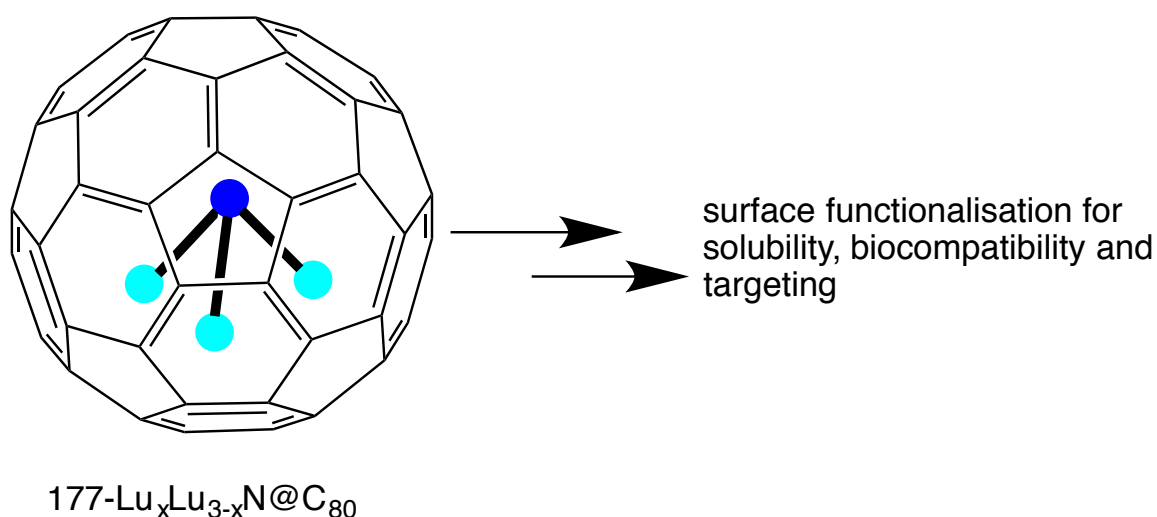


Figure 28. Cartoon representation of fullerene encapsulated ^{177}Lu .

Small diameter carbon nanospheres can be co-functionalised with an integrin targeting peptide cRGDfK and a ^{177}Lu labelled DOTA chelate (linked *via* a classical amide group).¹⁶³ Carbon nanospheres are attractive scaffolds as they are generally regarded as biologically benign and relatively inert. Interestingly, it is also possible to incorporate ^{177}Lu (specifically as $^{177}\text{Lu}_x\text{Lu}_{3-x}\text{N}@C_{80}$) inside a fullerene cage (Fig. 28).¹⁶⁴ The encapsulated $^{177}\text{Lu(III)}$ ions were not released for at least one half-life (6.7

days) showing the robustness of the system, and the fullerene was surface tagged with an interleukin-13 peptide. The mechanism for the loss of ^{177}Lu from the cage beyond this timescale has not been postulated, but assumed to proceed *via* radiolytic damage. The long-term stability of related Gd(III) species (e.g. gadofullerenes) that have potential in MRI has already been well documented.¹⁶⁵

7. Future prospects and untapped potential

When we consider the radioisotopes of the metallic elements, including the *f* block, the periodic table becomes very large indeed. The radiolanthanides offer rich and untapped opportunities for both imaging and therapeutic applications. The Ln(III) ions generally have similar chemistry (the only consideration being complexes of the larger lanthanides, early in the series, typically displaying slightly lower stability constants for a given ligand). Therefore, these isotopes offer the possibility of being used as a 'cocktail of ions' with a suitable ligand. This implies that α , β^- , β^+ and γ radiation may all be accessible, with some degree of choice on the energy and lifetime of the radioactive processes. More specifically, the radiolanthanides offer species emitting a high proportion of high energy penetrating radiation that are suitable for diagnostic applications (e.g. SPECT or PET), while other radiolanthanides emit non-penetrating particles (electrons or alpha particles), which are more suitable for therapeutic applications. Conveniently, some therapeutic radiolanthanides also emit penetrating photons which may be useful for the imaging of the therapeutic agent itself. Furthermore, the energy and hence range in tissue of these varying particles also needs careful consideration. For example, the variation in the energies of the beta particles between ^{90}Y (11 mm tissue penetration), ^{166}Ho (9 mm), ^{149}Pm (5 mm) and ^{177}Lu (2 mm), will have implications with regards to the size of tumour that a

therapeutic reagent should be matched with. Further still, one also needs to consider the half-life of the isotope, which should match the half-life of the final reagent. Clearly a therapeutic reagent which dissipates most of its energy before it reaches its biological target will do more harm than good. For example, Lewis and co-workers¹³⁶ reported a comparison of ^{149}Pm , ^{166}Ho and ^{177}Lu for use in CC49 radioimmunotherapy. With 96 h required to reach maximum tumour loading, the 26.9 h half-life of ^{166}Ho was not appropriate for conventional radioimmunotherapy. However, a pre-targeting strategy using streptavidin-labelled CC49, followed by a clearing reagent and then a biotin-labelled radiocomplex, allowed maximum tumour uptake in 4 h.¹⁶⁶ However, even with more favourable kinetics, the 9 mm range of ^{166}Ho was unsuitable for a 1 g tumour, with less radiative energy being delivered to the xenograft compared to the ^{149}Pm and ^{177}Lu analogues.

Although at first sight there are a large number of ligands that have been used to synthesise radiolanthanide complexes, closer inspection reveals a relatively narrow design philosophy based on (poly)aminophosphonates and (poly)aminocarboxylate derivatives. Clearly, several key ligand derivatives such as bone-targeting EDTMP, or DOTA and DTPA, are commercially available, often in functionalised form to allow further conjugation. As noted elsewhere, the choice of ligand should clearly be matched with the characteristics of the radiolanthanide. Consideration of thermodynamic stability should be balanced with the formation kinetics of such species; this is particularly important for the practicalities of the synthesis of radiopharmaceuticals. However, a caveat for this latter point are the advantages offered by the long half-lives of many of the viable radiolanthanides.

A frequent observation from a number of the studies described in this review is the lack of detail regarding the precise speciation of some of the ligand:radiolanthanide

species. This is particularly true of the work on acyclic aminophosphonate chelate derivatives where there is a paucity of information regarding speciation and stability constant data on non-radioactive analogues, as well as more traditional methods for coordination complex characterisation. We assume such issues partially explain why DTPA and DOTA-like chelates are so popular, as the Ln(III) coordination chemistry is assumed to be well defined and understood. However, there are several reports detailing the release of the metal ion from the DOTA framework over the course of the nuclear decay. An elucidation of the mechanism of this process is clearly hampered by the low concentrations of species involved and their hazardous nature. However, it is clear that a better understanding of this process may identify criteria for the design of new ligands and even allow the design of new materials which can positively utilise the released daughter ion in further down-stream applications.

The combination of radiolanthanides with nanoparticle and/or nanomaterial type structures appears to offer very rich design opportunities. This is particularly true when considering the opportunities presented by multimodality¹⁶⁷ approaches. While the *in vivo* or *in vitro* concentration regimes for radiolanthanide species would render them unsuitable for either MR or optical imaging work, supporting work on fluorescently labelled analogues could be a crucial tool in understanding species at the cellular level. Of course, the complexity of any assembly must be robust in a radiological sense, and it is interesting to note that there are approaches to reducing radiolysis.¹⁶⁸

Over the next decade researchers (across the physical and biological sciences) and clinicians can expect rapid development in the utility and application of radiolanthanides. This review has highlighted some of the key classes of chelating agents that are currently used, but there are clearly huge opportunities in the design

of new targeted systems that can match the radioactive properties of the lanthanide to the imaging and therapeutic targets.

References

- ¹ Handbook of Radiopharmaceuticals: Radiochemistry and Applications, Eds M.J. Welch, C.S. Redvanly, Wiley, New York 2005.
- ² C.S. Levin, E.J. Hoffman, *Phys. Med. Biol.* 44 (1999) 781–799.
- ³ F. Rosch, *Radiochim. Acta* 95 (2007) 303-311.
- ⁴ M. Neves, A. Kling, A. Oliveira, *J. Radioanal. Nucl. Chem.* 266 (2005) 377-384.
- ⁵ a) CRC Handbook of Chemistry and Physics. 84th ed. CRC Press: Boca Raton, FL, 2003-2004; b) National Nuclear Data Center, Brookhaven National Laboratory, Upton, N.Y., USA
- ⁶ M. Lubberink, H. Lundqvist, V. Tolmachev, *Physics in Medicine & Biology*, 47 (2002) 615-629; H.A. O'Brien, P.M. Grant, *Appl. Nucl. Radiochem.* (1982) 57-67.
- ⁷ S. Aime, A. Barge, F. Benetollo, G. Bombieri, M. Botta, F. Ugger, *Inorg. Chem.* 36 (1997) 4287-4289
- ⁸ K. Kobayashi, M. Kuwano, K. Sueki, K. Kikuchi, Y. Achiba, H. Nakahara, N. Kananishi, M. Watanabe, K. Tomura, *Journal of Radioanalytical and Nuclear Chemistry* 192 (1995) 81–89
- ⁹ K. P. Zhernosekov, D. V. Filosofov, S. M. Qaim, F. Rösch, *Radiochim. Acta*, 95 (2007) 319–327
- ¹⁰ D.E. Chambers, D.A. Parks, G. Patterson, R. Roy, J.M. McCord, S. Yoshida, L.F. Parmley, J.M. Downey, *J. Mol. Cell. Cardiol.* 17 (1985) 145-152.
- ¹¹ R.Q. Wu, W.F. Dong, M. Zhou, X.X. Cui, H.H. Simms, P. Wang, *Cardiovasc. Res.* 68 (2005) 318-326.
- ¹² O. Kallskog, M. Wolgast, H.R. Ulfendahl, *Acta Physiol. Scand.* 85 (1972) 408.

-
- ¹³ X. Guo, Q. Zhou, T. Lu, M. Fang, X. Huang, *Annals of Botany* 100(7) (2007) 1459-1465.
- ¹⁴ T.S. Pilgrim, R.J. Watling, K. Grice, *Food Chem.* 118 (2010) 921-926.
- ¹⁵ F. Soltani, A.B. Samani, M. Sadeghi, S.S. Arani, K. Yavari, *J. Radioanal. Nucl. Chem.* 303 (2015) 385-391.
- ¹⁶ D. K. Bhattacharyya, S. Basu, *Sep. Sci. Technol.* 11 (1976) 503
- ¹⁷ S.K. Imam, *Int. J. Radiat. Oncol. Biol. Phys.* 51 (2001) 271-278
- ¹⁸ <http://home.cern/about/experiments/isolde>
- ¹⁹ S. Lehenberger, C. Barkhausen, S. Cohrs, E. Fischer, J. Grunberg, A. Hohn, U. Koster, R. Schibli, A. Turler, K. Zhernosekov, *Nucl. Med. Biol.* 2011, 38, 917-924
- ²⁰ P. M. Grant, G. E. Montero, A. M. Newman, H.A. O'Brien Jr, *J. Radioanal. Nucl. Chem.* 96 (1985) 629
- ²¹ W. Liu, X. Li, Y. Wen, M. Tan, *Dalton Trans.* (2004) 640-644
- ²² For example: J-C. Bunzli, C. Piguet, *Chem. Soc. Rev.* 34 (2005) 1048-1077; K. Binnemans, *Chem. Rev.* 109 (2009) 4283-4374; E.J. New, D. Parker, D.G. Smith, J.W. Walton, *Curr. Opin. Chem. Biol.* 14 (2010) 238-246; A.J. Amoroso, S.J.A. Pope, *Chem. Soc. Rev.* 44 (2015) 4723-4742; S. Faulkner, B.P. Burton-Pye, S.J.A. Pope, *Appl. Spec.* 40 (2005) 1-31.
- ²³ R.D. Teo, J. Termini, H.B. Gray, *J. Med. Chem.* 59 (2016) 6012-6024.
- ²⁴ W.A. Volkert, T.J. Hoffman, *Chem. Rev.* 99 (1999) 2269-2292
- ²⁵ F. Rosch, R.P. Baum, *Dalton Trans.* 40 (2011) 6104-6111
- ²⁶ J.M. van Dodewaard-de Jong, D.E. Oprea-Lager, L. Hooft, J.M.H. de Klerk, H.J. Bloemendal, H.M.W. Verheul, O.S. Hoekstra, A.J.M. van den Eertwegh, *Eur. Urology* 70 (2016) 416-426.
- ²⁷ S. Banerjee, M.R.A. Pillai, F.F. Knapp, *Chem. Rev.* 115 (2015) 2934-2974.

-
- ²⁸ V.K. Tishchenko, V.M. Petriev, V.G. Skvortsov, *Pharmaceutical Chem. J.* 49 (2015) 425-431.
- ²⁹ R. Lange, R. ter Heine, F.F. Knapp, J.M.H. de Klerk, H.J. Bloemendal, N.H. Hendrikse, *Bone* 91 (2016) 159-179
- ³⁰ G. Bauman, M. Charette, R. Reid, J. Sathya, *Radiotherapy and Oncology* 75 (2005) 258-271; I.G. Finlay, M.D. Mason, M. Shelley, *Lancet Oncol.* 6 (2005) 392-400.
- ³¹ I.A. Abbasi, *Nucl. Med. Biol.* 39 (2012) 763-769.
- ³² P. Anderson, R. Nunez, *Expert Rev. Anticancer Ther.* 7 (2007) 1517-1527
- ³³ Y. Yang, M.J. Pushi, D.M.L. Cooper, M.R. Doschak, *Mol. Pharmaceutics* 12 (2015) 4108-4114.
- ³⁴ E. Prinz, I. Szilagyi, K. Mogyrosi, I. Labadi, *J. Therm. Anal. Cal.* 69 (2002) 427-439
- ³⁵ F.K. Kalman, R. Kiraly, E. Brucher, *Eur. J. Inorg. Chem.* (2008) 4719-4727
- ³⁶ A. Mondry, R. Janicki, *Dalton Trans.* (2006) 4702-4710.
- ³⁷ J.A. Kalef-Ezra, S.T. Valakis, S. Pallada, *Physica Medica* 31 (2015) 104-107.
- ³⁸ G.J. Beyer, R. Offord, G. Kunzi, Y. Aleksandrova, U. Ravn, S. Jahn, J. Barker, O. Tengblad, M. Lindroos, *Nucl. Med. Biol.* 24 (1997) 367-372.
- ³⁹ T. Das, S. Chakraborty, H.D. Sarma, P. Tandon, S. Banerjee, M. Venkatesh, M.R.A. Pillai, *Nucl. Med. Biol.* 36 (2009) 561-568
- ⁴⁰ S. Chakraborty, T. Das, H.D. Sarma, M. Venkatesh, S. Banerjee, *Appl. Rad. Isotop.* 66 (2008) 1196.
- ⁴¹ B. Mathew, S. Chakraborty, T. Das, H.D. Sarma, S. Banerjee, G. Samuel, M. Venkatesh, M.R.A. Pillai, *Appl. Rad. Isotop.* 60 (2004) 635-642.

-
- ⁴² M.A. Majali, A.R. Mathakar, H.H. Shimpi, S. Banerjee, G. Samuel, Appl. Rad. Isotop. 53 (2000) 987-991.
- ⁴³ I. Kubalek, O. Fain, J. Paries, A. Kettaneh, M. Thomas, Rheumatology 40 (2001) 1394-1397
- ⁴⁴ <http://www.pharma.us.novartis.com/product/pi/pdf/aredia.pdf>
- ⁴⁵ M. Neves, L. Gano, N. Pereira, M.C. Costa, M.R. Costa, M. Chandia, M. Rosado, R. Fausto, Nucl. Med. Biol. 29 (2002) 329-338.
- ⁴⁶ E. Guenin, M. Monteil, N. Bouchemal, T. Prange, M. Lecouvey, Eur. J. Org. Chem. (2007) 3380-3391.
- ⁴⁷ A. Fakhari, A.R. Jalilian, H. Yousefnia, F. Johari-Daha, M. Mazidi, A. Khalaj, J. Radioanal. Nucl. Chem. 303 (2015) 743-750.
- ⁴⁸ R. Fu, S. Hu, X. Wu, Cryst. Growth Des. 14 (2014) 6197-6204
- ⁴⁹ M. Arabieh, M.H. Khodabandeh, M.H. Karimi-Jafari, C. Platas-Iglesias, K. Zare, J. Rare Earths 33 (2015) 310-319.
- ⁵⁰ A. Wardley, N. Davidson, P. Barrett-Lee, A. Hong, J. Mansi, D. Dodwell, R. Murphy, T. Mason, D. Cameron, British Journal of Cancer 92 (2005) 1869-1876
- ⁵¹ J. Lin, L. Qiu, W. Cheng, S. Luo, L. Xue, S. Zhang, Appl. Radiat. Isot. 70 (2012) 845-855
- ⁵² K. McKenzie, M. Eng, J.D. Bobyn, J. Roberts, D. Karabasz, M. Tanzer, Clin. Orthop. Relat. Res. 469 (2011) 514-522
- ⁵³ M. Nikzad, A.R. Jalilian, S. Shirani-Arani, A. Bahrami-Samani, H. Golchoubian, J. Radioanal. Nucl. Chem. 298 (2013) 1273-1281.
- ⁵⁴ M.G.E.H. Lam, A. Dahmane, W.H.M. Stevens, P.P. van Rijk, J.M.H. de Klerk, B.A. Zonnenberg, Eur. J. Nucl. Med. Mol. Imaging 35 (2008) 756-765.

-
- ⁵⁵ J.R. Zeevart, N.V. Jarvis, W.K.A. Louw, G.E. Jackson, J. Inorg. Biochem. 83 (2001) 57-65
- ⁵⁶ M.E. Mewis, S.J. Archibald, Coord. Chem. Rev. 254 (2010) 1686-1712; T.W. Price, J. Greenman, G.J. Stasiuk, Dalton Trans. 45 (2016) 15702; E.W. Price, C. Orvig, Chem. Soc. Rev. 43 (2014) 260.
- ⁵⁷ I. Lukes, J. Kotek, P. Vojtisek, P. Hermann, Coord. Chem. Rev. 216-217 (2001) 287-312
- ⁵⁸ A.D. Sherry, J. Ren, J. Huskens, E. Brucher, E. Toth, C.F.C.G. Geraldes, M.M.C.A. Castro, W.P. Cacheris, Inorg. Chem. 35 (1996) 4604-4612.
- ⁵⁹ T. Das, S. Chakraborty, P.R. Unni, S. Banerjee, G. Samuel, H.D. Sarma, M. Venkatesh, M.R.A. Pillai, Appl. Rad. Isotop. 57 (2002) 177-184.
- ⁶⁰ K.V. Vimalnath, A. Rajeswari, H.D. Sarma, S. Chakraborty, Nuclear Medicine and Biology 41(7) (2014) 634-634.
- ⁶¹ R. Bergmann, M. Meckel, V. Kubicek, J. Pietzsch, J. Steinbach, P. Hermann, F. Rosch, EJNMMI Research 6 (2016) 5-17
- ⁶² M.P.C. Campello, S. Lacerda, I.C. Santos, G.A. Pereira, C.F.G.C. Geraldes, J. Kotek, P. Hermann, J. Vaněk, P. Lubal, V. Kubíček, É. Tóth, I. Santos Chemistry—A European Journal, 16 (2010) 8446-8465.
- ⁶³ M.P. Campello, F. Marques, L. Gano, S. Lacerda, I. Santos, Radiochimica Acta, 95 (2007) 329-334
- ⁶⁴ S. Lacerda, M.P. Campello, F. Marques, L. Gano, I. Santos, Metal Ions In Biol. Med., 9 (2006) 46-51
- ⁶⁵ G. Hao, W. Liu, G. Hassan, O.K. Öz, Z. Kovacs, X. Sun, Bioorg. Med. Chem. Lett., 25 (2015) 571-4

-
- ⁶⁶ F. Marques, L. Gado, M.P. Campello, S. Lacerda, I. Santos, L.M.P. Lima, J. Costa, P. Antunes, R. Delgado, J. Inorg. Biochem. 100 (2006) 270-280.
- ⁶⁷ C. Rill, Z.I. Kolar, G. Kickelbick, H.Th. Wolterbeek, J.A. Peters, Langmuir, 25 (2009) 2294-2301.
- ⁶⁸ J. Rudovsky, J. Kotek, P. Hermann, I. Lukes, V. Mainero, S. Aime, Org. Biomol. Chem. 3 (2005) 112-117.
- ⁶⁹ S. Lacerda, F. Marques, P. Campello, L. Gano, V. Kubicek, P. Hermann, I. Santos, J. Label Compd. Radiopharm 53 (2010) 36-43.
- ⁷⁰ F. Marques, K.P. Guerra, L. Gano, J. Costa, M.P. Campello, L.M.P. Lima, R. Delgado, I. Santos, J. Biol. Inorg. Chem., 9 (2004) 859.
- ⁷¹ M.P. Campello, F. Marques, L. Gano, S. Lacerda, I. Santos, Radiochimica Acta, 95 (2007) 329-334
- ⁷² D.J. Bornhop, D.S. Hubbard, M.P. Houlne, C. Adair, G.E. Kiefer, B.C. Pence, D.L. Morgan, Anal. Chem. 71 (1999) 2607-2615.
- ⁷³ M.P. Houlne, T.S. Agent, G.E. Kiefer, K. Mcmilan, D.J. Bornhop, Appl. Spectrosc. 50 (1996) 1221
- ⁷⁴ M. Le Fur, M. Beyler, N. Lepareur, O. Fougere, C. Platas-Iglesias, O. Rousseaux, R. Tripier, 55 (2016) 8003-8012.
- ⁷⁵ J. Notni, J. Simecek, H-J. Wester, ChemMedChem 9 (2014) 1107-1115.
- ⁷⁶ J. Broan, K. J. Jankowski, R. Katakya, D. Parker, J. Chem. Soc. Chem. Commun. (1990) 1738 – 1739; E. Cole, D. Parker, G. Ferguson, J. F. Gallagher, B. Kaitner, J. Chem. Soc. Chem. Commun. (1991) 1473 – 1475
- ⁷⁷ For example, M. Soulie, F. Latzko, E. Bourrier, V. Placide, S.J. Butler, R. Pal, J.W. Walton, P.L. Baldeck, B. Le Guennic, C. Andraud, J.M. Zwieter, L. Lamargue, D. Parker, O. Maury, Chem. Eur. J. 20 (2014) 8636-8646; J.W. Walton, A. Bourdolle,

-
- S.J. Butler, M. Soulie, M. Delbianco, B.K. McMahon, R. Pal, H. Puschmann, J.M. Zwier, L. Lamarque, O. Maury, C. Andraud, D. Parker, *Chem. Commun.* 49 (2013) 1600-1602.
- ⁷⁸ A.T. Bui, A. Grichine, S. Brasselet, A. Duperray, C. Andraud, O. Maury, *Chem. Eur. J.* 21 (2015) 17757-17761.
- ⁷⁹ A.M. Nonat, C. Gateau, P.H. Fries, L. Helm, M. Mazzanti, *Eur. J. Inorg. Chem.* 2012, 2049-2061.
- ⁸⁰ G.J. Stasiuk, N.J. Long, *Chem. Commun.* 49 (2013) 2732-2746.
- ⁸¹ L.M. de Leon-Rodriguez, Z. Kovacs, *Bioconjug. Chem.* 19 (2008) 391-402.
- ⁸² W. L. Grovum, V. J. Williams, *British Journal of Nutrition*, 30, (1973) 313–329.
- ⁸³ W.P. Cacheris, S.K. Nickle, A.D. Sherry, *Inorg. Chem.* 26 (1987) 958-960.
- ⁸⁴ K. Kumar, C.A. Chang, M.F. Tweedle, *Inorg. Chem.* 32 (1993) 587-593.
- ⁸⁵ P. Caravn, J.J. Ellison, T.J. McMurry, R.B. Lauffer, *Chem. Rev.* 99 (1999) 2293.
- ⁸⁶ T. Kanda, H. Oba, K. Toyoda, K. Kitajima, S. Furui, *Jpn. J. Radiol.* 34 (2016) 3-9.
- ⁸⁷ P. Wedeking, M. Tweedle, *Int. J. Radiat. Appl. Instrum. B* 15 (1988) 395-402
- ⁸⁸ M.F. Tweedle, P. Wedeking, K. Kumar, *Invest. Radiol.* 30 (1995) 372-380.
- ⁸⁹ K. Kumar, K. Sukumaran, C.A. Chang, M.F. Tweedle, W.C. Eckelman, *J. Labl. Comp. Radiopharm.* 33 (1993) 473-482.
- ⁹⁰ S. Torres, J.A. Martins, J.P. Andre, M. Neves, A.C. Santos, M.I.M. Prata, C.F.G.C. Geraldes, *Radiochimica Acta* 95 (2007) 343-349.
- ⁹¹ G. Tircso, Z. Kovacs, A.D. Sherry, *Inorg. Chem.* 45 (2006) 9269-9280.
- ⁹² G. Tircso, E. T. Benyo, E.H. Suh, P. Jurek, G.E. Kiefer, A.D. Sherry, Z. Kovacs, *Bioconjugate Chem.* 20 (2009) 565-575.
- ⁹³ G.A. bailey, E.W. Price, B.M. Zeglis, C.L. Ferreira, E. Boros, M.J. Lacasse, B.O. Patrick, J.S. Lewis, M.J. Adam, C. Orvig, *Inorg. Chem.* 51 (2012) 12575-12589

-
- ⁹⁴ P.A. Waghorn, J. Label Compd. Radiopharm. 57 (2014) 304-309
- ⁹⁵ C-P. Wong, R.F. Venteicher, W. DeW. Horrocks Jr. J. Am. Chem. Soc. 96 (1974) 7149.
- ⁹⁶ W. DeW. Horrocks Jnr., C-P. Wong, J. Am. Chem. Soc. 98 (1976) 7157-7160
- ⁹⁷ J. Pan, B.I. Harriss, C-F. Chan, L. Jiang, T-H. Tsoi, N.J. Long, W-T. Wong, W-K. Wong, K-L. Wong, Inorg. Chem. 55 (2016) 6839-6841
- ⁹⁸ A.F. Mironov, Russ. Chem. Rev. 82 (2013) 333-351.
- ⁹⁹ N. Vahidfar, A.R. Jalilian, Y. Fazaeli, A. Bahrami-Samani, D. Beiki, A. Khalaj, J. Radioanal. Nucl. Chem. 301 (2014) 269-276.
- ¹⁰⁰ N. Vahidfar, R. Amir, A.R. Jalilian, Y. Fazaeli, A. Bahrami-Samani, D. Beiki, A. Khalaj, J. Radioanal. Nucl. Chem. 295 (2013) 979-986.
- ¹⁰¹ M. Aboudzadeh, Y. Fazaeli, H. Khodaverdi, H. Afarideh, J. Radioanal. Nucl. Chem. 295 (2013) 105-113.
- ¹⁰² V. Bulach, F. Sguerra, M.W. Hosseini, Coord. Chem. Rev. 256 (2012) 1468-1478.
- ¹⁰³ H-S. He, Z-X. Zhao, W-K. Wong, K-F. Li, J-X. Meng, K-W. Cheah, Dalton Trans. (2003) 980
- ¹⁰⁴ O.J. Stacey, S.J.A. Pope, RSC Adv. 3 (2013) 25550-25564
- ¹⁰⁵ M. Guleria, T. Das, H.D. Sarma, S. Banerjee J. Radioanal. Nucl. Chem. 307 (2016) 1537-1544
- ¹⁰⁶ L.M. de Leon-Rodriguez, Z. Kovacs, Bioconjugate Chem. 19 (2008) 391-402.
- ¹⁰⁷ For example, D.J. Kwekkeboom, W.H. Bakker, B.L. Kam, J.J.M. Teunissen, P.P.M. Kooij, W.W. de Herder, R.A. Feelders, C.H.J. van Eijck, N. de Jong, A. Srinivasan, J.L. Erion, E.P. Krenning, Eur. J. Nucl. Med. Mol. Imaging 30 (2003) 417-422; D.J. Kwekkeboom, J.J. Teunissen, W.H. Bakker, P.P. Kooij, W.W. de Herder, R.A. Fielders, M.O. van Aken, E.P. Krenning, J. Clin. Oncol. 23 (2005) 2754-2762

-
- ¹⁰⁸ E.R. Balkin, D. Liu, F. Jia, V.C. Ruthengael, S.M. Shaffer, W.H. Miller, M.R. Lewis, Nucl. Med. Biol. 41 (2014) 36-42.
- ¹⁰⁹ A. Ianniello, M. Sansovini, S. Severi, S. Nicolini, C.M. Grana, K. Massri, A. Bongiovanni, L. Antonuzzo, V. Di Iorio, A. Sarnelli, P. Caroli, M. Monti, E. Scarpi, G. Paganelli, Eur. J. Nucl. Med. Mol. Imaging 43 (2016) 1040-1046
- ¹¹⁰ C. Muller, E. Fischer, M. Behe, U. Koster, H. Dorrer, J. Reber, S. Haller, S. Cohrs, A. Blanc, J. Grunberg, M. Bunka, K. Zhernosekov, N. Van der Meulen, K. Johnston, A. Turler, R. Schibli, Nucl. Med. Boil., 2014, 41, e58-e65.
- ¹¹¹ C. Schuchardt, H.R. Kulkarni, V. Prasad, C. Zachert, D. Muller, R.P. Baum, Recent Results Cancer Res. 194 (2013) 519
- ¹¹² C. Muller, C. Vermeulen, K. Johnston, U. Koster, R. Schmid, A. Turler, N.P. van der Meulen, EJNMMI Research 6 (2016) 35.
- ¹¹³ C. Muller, C. Vermeulen, U. Koster, K. Johnston, A. Turler, R. Schibli, N.P. van der Meulen, EJNMMI, 2016, 1:5.
- ¹¹⁴ J.C. Lim, E.H. Cho, J.J. Kim, S.M. Choi, S.Y. Lee, S.S. Nam, U.J. Park, S.H. Park, Nuclear Med. Biol. 42 (2015) 131-136
- ¹¹⁵ F. Hu, C.S. Cutler, T. Hoffman, G. Sieckman, W.A. Volkert, S.S. Jurisson, Nucl. Med. Biol. 29 (2002) 423-430
- ¹¹⁶ C. Müller, K. Zhernosekov, U. Köster, K. Johnston, H. Dorrer, A. Hohn, N.T. van der Walt, A. Turler, R. Schibli, J Nucl Med. 2012, 53,1951-9.
- ¹¹⁷ R.M. dos Santos Augusto, L. Buehler, Z. Lawson, S. Marzari, M. Stachura, T. Stora Appl. Sci. 2014, 4, 265-281.
- ¹¹⁸ B. Ballard, Z. Jiang, C.E. Soll, E. Revskaya, C.S. Cutler, E. Dadachova, L.C. Francesconi Cancer Biother. Radiopharm. 26 (2011) 547-556
- ¹¹⁹ D. Parker, Chem. Soc. Rev. 19 (1990) 271-291.

-
- ¹²⁰ M. Vosjan, L.R. Perk, G.W.M. Visser, M. Budde, P. Jurek, G.E. Kiefer, G. van Dongen, *Nature Protocols* 5(4) (2010) 739-743.
- ¹²¹ M. Kameswaran, U. Pandey, N. Gamre, K.V. Vimalnath, H.D. Sarma, A. Dash, *Appl. Rad. Isotop.* 114 (2016) 196-201.
- ¹²² M.E. Izard, G.R. Boniface, K.L. Hardiman, M.W. Brechbiel, O.A. Gansow, K.Z. Walkers, *Bionjugate Chem.* 3 (1992) 346-350.
- ¹²³ G.L. Plosker, D.P. Figgitt, *Drugs* 63 (2003) 803-843.
- ¹²⁴ F. Forrer, J. Chen, M. Fani, P. Powell, A. Lohri, J. Muller-Brand, *Eur. J. Nucl. Med. Mol. Imaging* 36 (2009) 1443-1452.
- ¹²⁵ P.F. Audicio, G. Castellano, M.R. Tassano, M.E. Rezzano, M. Fernandez, E. Riva, A. Robles, P. Cabral, H. Balter, P. Oliver, *Appl. Rad. Isotop.* 69 (2011) 924-928.
- ¹²⁶ U. Pandey, M. Kameswaran, H.D. Sarma, G. Samuel, *Appl. Radiat. Isot.* 86 (2014) 52-56
- ¹²⁷ A.R. Jalilian, L. Mirsadeghi, R. Haji-Hosseini, *J. Radioanal. Nucl. Chem.* 274 (2007) 175-179.
- ¹²⁸ M. Kameswaran, U. Pandey, C. Dhakan, K. Pathak, V. Gota, K.V. Vimalnath, A. Dash, G. Samuel, *Cancer Biother. Radiopharm.* 30 (2015) 240-246.
- ¹²⁹ A. Bahrami-Samani, M. Ghannadi-Maragheh, A.R. Jalilian, H. Yousefnia, J. Garousi, S. Moradkhani, *Nukleonika*, 54 (2009) 271-277.
- ¹³⁰ G.J. Beyer, M. Miederer, S. Vranješ-Đurić, J. J. Čomor, G. Künzi, O. Hartley, R. Senekowitsch-Schmidtke, D. Soloviev, F. Buchegger, *Eur. J. Nucl. Med. Mol. Imaging*, 2004, 31, 547-54
- ¹³¹ S. Thompson, B. Ballard, Z. Jiang, E. Revskaya, N. Sisay, W.H. Miller, C.S. Cutler, E. Dadachova, L.C. Francesconi, *Nucl. Med. Biol.* 41 (2014) 276-281.

-
- ¹³² T. Weber, B. Botticher, W. Mier, M. Sauter, S. Kramer, K. Leotta, A. Keller, A. Schlegelmilch, L. Grosse-Hovest, D. Jager, U. Haberkorn, M.A.E. Arndt, J. Krauss, *Eur. J. Nucl. Med. Mol. Imag.* 43 (2016) 489-498.
- ¹³³ S. Lacerda, M.P. Campello, F. Marques, L. Gado, V. Kubicek, P. Fouskova, E. Toth, I. Santos, *Dalton Trans.* (2009) 4509-4518.
- ¹³⁴ H. Mohsin, F. Jia, G. Sivaguru, M.J. Hudson, T.D. Shelton, T.J. Hoffman, C.S. Cutler, A.R. Ketring, P.S. Athey, J. Simon, R.K. Frank, S.S. Jurisson, M.R. Lewis, *Bioconjugate Chem.* 7 (2006) 485-492
- ¹³⁵ W.P. Li, D.S. Ma, C. Higginbotham, T. Hoffman, A.R. Ketring, C.S. Cutler, S.S. Jurisson, *Nucl. Med. Biol.* 28 (2001) 145-154
- ¹³⁶ H. Mohsin, F. Jia, J.N. Bryan, G. Sivaguru, C.S. Cutler, A.R. Ketring, W.H. Miller, J. Simon, R.K. Frank, L.J. Theodore, D.B. Axworthy, S.S. Jurisson, M.R. Lewis, *Bioconjugate Chem.* 22 (2011) 2444-2452
- ¹³⁷ S. Liu, T.D. Harris, C.E. Ellars, D.S. Edwards, *Bioconjugate Chem.* 14 (2003) 1030-1037.
- ¹³⁸ M-H. Pan, D-W. Gao, J. Feng, J. He, Y. Seo, J. Tedesco, J.G. Wolodzko, B.H. Hasegawa, B.L. Franc, *Mo. Imaging Biol.* 11 (2009) 159-166.
- ¹³⁹ K. Knogler, J. Grunberg, I. Novak-Hofer, K. Zimmermann, P.A. Schubiger, *Nucl. Med. Biol.* 33 (2006) 883-889.
- ¹⁴⁰ C. Muller, H. Struthers, C. Winiger, K. Zhernosekov, R. Schibli, *J. Nucl. Med.* 54 (2013) 124-131.
- ¹⁴¹ H-S. Chong, D. E. Milenic, K. Garmestani, E. D. Brady, H. Arora, C. Pfiester, M. W. Brechbiel, *Nucl. Med. Biol.* 33 (2006) 459-467; H-S. Chong, H.A. Song, N. Birch, T. Le, S. Lim, X. Ma, *Bioorg. Med. Chem. Lett.* 18 (2008) 3436-3439

-
- ¹⁴² H-S. Chong, H.A. Song, C.S. Kang, T. Le, X. Sun, M. Dadwal, H. Lee, X. Lan, Y. Chen, A. Dai, *Chem. Commun.* 47 (2011) 5584-5586.
- ¹⁴³ C.S. Kang, X. Sun, F. Jia, H.A. Song, Y. Chen, M. Lewis, H-S. Chong, *Bioconjugate Chem.* 23 (2012) 1775-1782.
- ¹⁴⁴ D.R.B. Vera, S. Eigner, K.E. Henke, O. Lebeda, F. Melichar, M. Beran, *Nucl. Med. Biol.* 39 (2012) 3-13.
- ¹⁴⁵ E.W. Price, B.M. Zeglis, J.F. Cawthray, C.F. Ramogida, N. ramos, J.S. Lewis, M.J. Adam, C. Orvig, *J. Am. Chem. Soc.* (135) 2013 12707-12721
- ¹⁴⁶ E.W. Price, B.M. Zeglis, J.F. Cawthray, J.S. Lewis, M.J. Adam, C. Orvig, *Inorg. Chem.* 53 (2014) 10412-10431.
- ¹⁴⁷ A.L.B. de Branco, A. Tsourkas, B. Saboury, V.N. Cardoso, A. Alavi, *EJNMMI Research* 2 (2012) 39
- ¹⁴⁸ S. Yook, Z. Cai, Y. Lu, M.A. Winnik, J-P. Pignol, R.M. Reilly, *Mol. Pharmaceutics* 12 (2015) 3963-3972
- ¹⁴⁹ S. Yook, Z. Cali, Y. Lu, M.A. Winnik, J-P. Pignol, R.M. Reilly, *J. Nucl. Med.* 57 (2016) 936-942.
- ¹⁵⁰ S. Yook, Y. Lu, J.J. Jeong, Z. Cai, L. Tong, R. Alwarda, J-P. Pignol, M.A. Winnik, R.M. Reilly, *Biomacromolecules* 17 (2016) 1292-1302
- ¹⁵¹ S. Shanehsazzadeh, C. Grüttner, H. Yousefnia, A. Lahooti, A. Gholami, S. Nosrati, S. Zolghadri, S. H. M. Anijdan, A. Lotfabadi, B.S. Varnamkhasti, F.J. Daha, A.R. Jalilian, *Radiochim. Acta*, 2016, DOI 10.1515/ract-2015-2499
- ¹⁵² G. Arora, J. Shukla, S. Ghosh, S.K. Maulik, A. Malhotra, G. Bandopadhyaya, *PLoS ONE* 7 (2012) e34019
- ¹⁵³ F. Danhier, E. Ansorena, J.M. Silva, R. Coco, A. Le Breton, V. Preat, *J. Control. Release* 161 (2012) 505-522

-
- ¹⁵⁴ G. Arora, P. Dubey, J. Shukla, S. Ghosh, G. Bandopadhyaya, *Ann. Nucl. Med.* 30 (2016) 334-345
- ¹⁵⁵ Y-L.J. Han, S.C.J. Loo, N.T. Phung, F. Boey, J. Ma, *J. Mater. Sci: Mater. Med.* 19 (2008) 2993-3003.
- ¹⁵⁶ Y. Peng, Y. Sun, L. Zhao, Y. Wu, W. Feng, Y. Gao, F. Li, *Biomaterials* 34 (2013) 9535-9544.
- ¹⁵⁷ I. Munaweera, D. Levesque-Bishop, Y. Shi, A.J. Di Pasqua, K.J. Balkus Jr. *ACS Appl. Mater. Interfaces* 2014, 6, 22250-22256.
- ¹⁵⁸ L. Jing, J. Shi, D. Fan, Y. Li, R. Liu, Z. Dai, F. Wang, J. Tian, *ACS Appl. Mater. Interfaces* 7 (2015) 22095-22105.
- ¹⁵⁹ F. Simonelli, P. Marmorato, K. Abbas, J. Ponti, J. Kozempel, U. Holzwarth, F. Franchini, F. Rossi, *IEEE Transactions on Nanobioscience* 10 (2011) 44-50.
- ¹⁶⁰ L. Yang, G. Sundaresan, M. Sun, P. Jose, D. Hoffman, P.R. McDonagh, N. Lamichhane, C.S. Cutler, J.M. Perez, J. Zweit, *J. Mater. Chem. B* 1 (2013) 1421.
- ¹⁶¹ J. You, J. Zhao, X. Wen, C. Wu, Q. Huang, F. Guan, R. Wu, D. Liang, C. Li, *J. Control. Release* 202 (2015) 40-48.
- ¹⁶² S. Chakraborty, K.S. Sharma, A. Rajeswari, K.V. Vimalnath, H.D. Sarma, U. Pandey, Jagannath, R.S. Ningthoujam, R.K. Vatsa, A. Dash, *J. Mater. Chem. B* 3 (2015) 5455-5466.
- ¹⁶³ D. Satpati, A. Satpati, Y. Pamale, C. Kumar, R. Sharma, H.D. Sarma, S. Banerjee, *RSC Adv.* 6 (2016) 50761-50769
- ¹⁶⁴ M.D. Schultz, J.C. Duchamp, J.D. Wilson, C-Y. Shu, J. Ge, J. Zhang, H.W. Gibson, H.L. Fillmore, J.I. Hirsch, H.C. Dorn, P.P. Fatouros, *J. Am. Chem. Soc.* 132 (2010) 4980-4981

¹⁶⁵ T. Li, S. Murphy, B. Kiselev, K.S. Bakshi, J. Zhang, A. Eltahir, Y. Zhang, Y. Chen, J. Zhu, R.M. Davis, L.A. Madsen, J.R. Morris, D.R. Karolyi, S.M. LaConte, Z. Sheng, H.C. Dorn, J. Am. Chem. Soc. 137 (2015) 7881-7888.

¹⁶⁶ M.R. Lewis, J. Zhang, F. Jia, N.K. Owen, C.S. Cutler, M.F. Embree, J. Schultz, L.J. Theodore, A.R. Ketring, S.S. Jurisson, D.B. Axworthy, Nucl. Med. Biol. 31 (2004) 213-223.

¹⁶⁷ L.E. Jennings, N.J. Long, Chem. Commun. (2009) 3511-3524.

¹⁶⁸ E. de Blois, H.S. Chan, M. Konijnenberg, R. de Zanger, W.A. Breeman, Curr. Top. Med. Chem. 12 (2012) 2677-2685